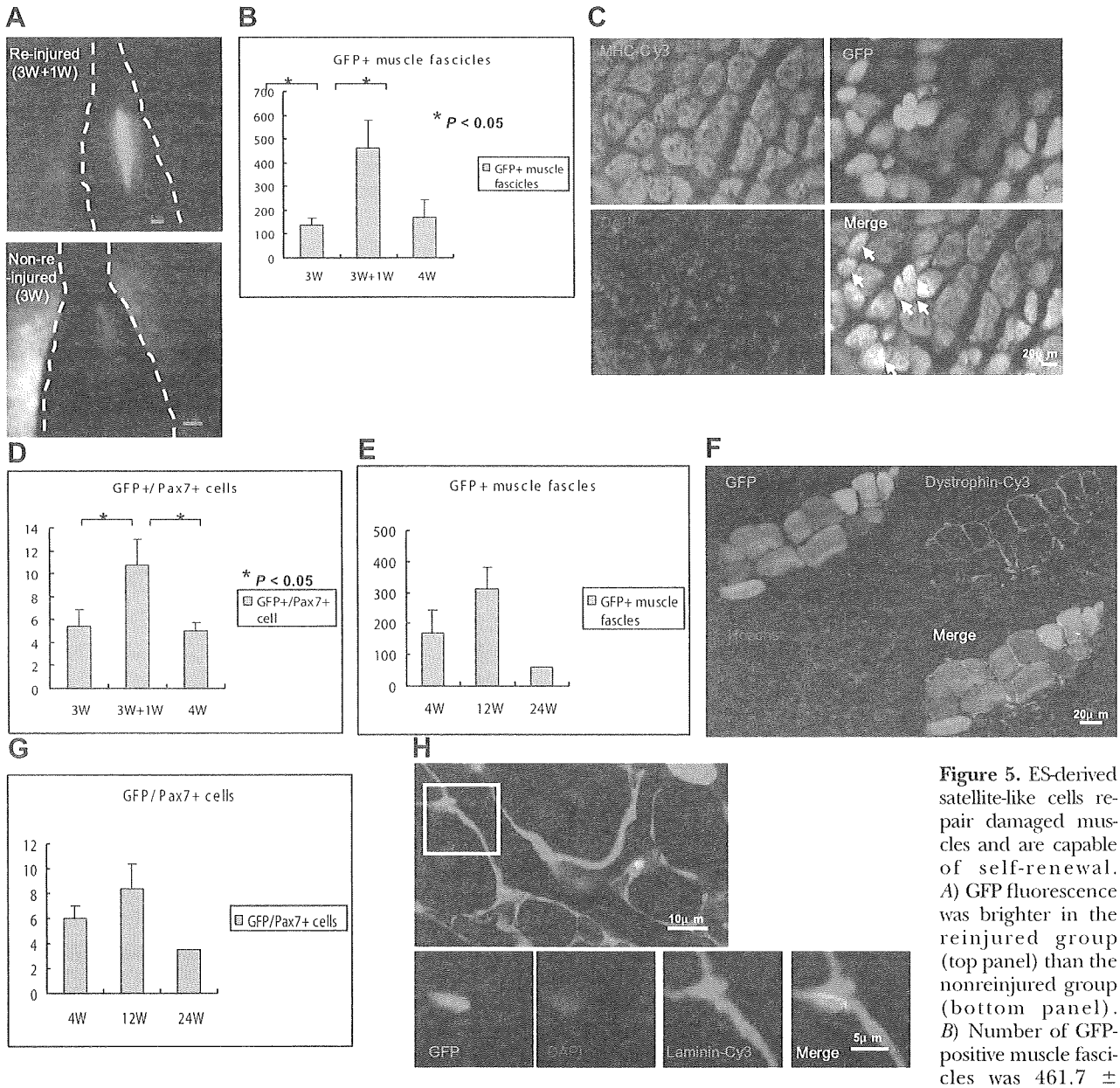

Figure 5. ES-derived satellite-like cells repair damaged muscles and are capable of self-renewal. *A*) GFP fluorescence was brighter in the reinjured group (top panel) than the nonreinjured group (bottom panel). *B*) Number of GFP-positive muscle fascicles was 461.7 ± 117.3 in the reinjured group (3W+1W) and 136.7 ± 27.9 and 168.7 ± 72.9 in the nonreinjured group at 3 wk (3W) and 4 wk (4W), respectively. *C*) GFP-positive fibers were confirmed to be MHC positive and contained central nuclei (arrows). *D*) Number of GFP/Pax7-double-positive cells also increased significantly in the reinjured group (10.8±3.0 cells at 3W+1W) compared to the nonreinjured group (5.4±1.2 and 6.0±1.0 at 3W and 4W, respectively). *E*) In long-term evaluations, number of GFP-positive muscle fascicles at 12 wk (12W) increased relative to number at 4 wk after transplantation [312.6±68.7 (n=3) *vs.* 168.7±72.9]. However, a decrease was observed at 24 wk (58.6; n=1). *F*) Immunostaining showed dystrophin (red) surrounding the donor-derived GFP-positive fibers (green), 24 wk after transplantation of SM/C-2.6-positive cells. *G*) Results similar to *E* were observed with the number of GFP/Pax7-double-positive cells. *H*) A GFP-positive cell beneath the basal lamina was observed. Scale bars = 1 mm (*A*); 20 μm (*C*); 20 μm (*F*); 10 μm (*H*, top panel); 5 μm (*H*, bottom panels).

like cells function as normal stem cells in skeletal muscle, they should be able to reside within the tissue for long periods of time and undergo asymmetric cell divisions to maintain the number of satellite cells and to generate muscle fibers. To examine this stem cell function, we analyzed the recipient mice at 4, 12, and 24 wk after transplantation. Intriguingly, in the LTA muscle of mdx mice transplanted with SM/C-2.6-positive cells, the number of GFP-positive fascicles at 12 wk increased over that at 4 wk [12.6±68.7 (n=3) *vs.* 168.7±72.9; Fig. 5*E*] but decreased by 24 wk (58.6; n=1). These engrafted GFP-positive tissues were confirmed to be MHC positive through immunostaining (Supplemental Fig. 9), and surrounding these GFP-positive fibers, dystrophin was observed (Fig. 5*F*). The numbers of GFP/Pax7-double-positive cells were maintained from week 4 to week 24 (Fig. 5*G*, Table 1, and Supplemental Fig. 10) and the location of GFP-positive cells under the basal lamina meets the anatomical definition of satellite cells (Fig. 5*H*). No teratomas were

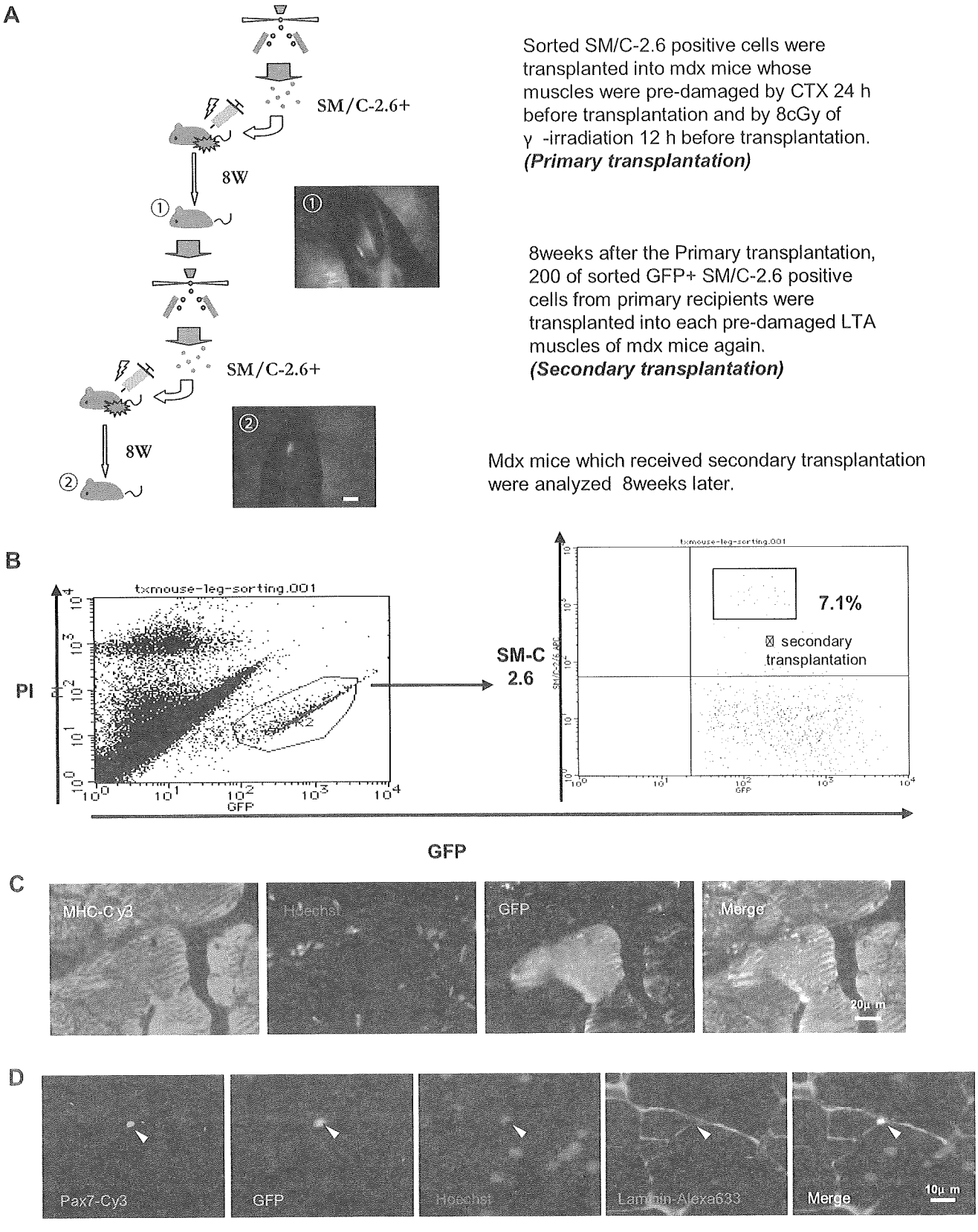

Figure 6. ES-derived satellite-like cells can be secondarily transplanted. *A*) SM/C-2.6-positive cells (2.5×10^4) were transplanted into the LTA muscle of recipient mice in primary transplantation, and as few as 200 SM/C-2.6-positive cells collected from the primary recipients were retransplanted (secondary transplantation) into the LTA muscle of secondary recipient mice. *B*) FACS data of primary transplantation indicated that 7.1% of engrafted (GFP-positive) cells were SM/C-2.6-positive. *C*) Eight weeks after secondary transplantation, immunostaining of LTA muscle for MHC showed that engrafted ES-derived GFP-positive tissues formed mature skeletal muscle fibers. *D*) GFP/Pax7-double-positive cells (arrowhead) located beneath the basal lamina were observed within GFP-positive LTA muscle of secondary recipient mice. Scale bars = 2 mm (*A*); 20 μm (*C*); 10 μm (*D*).

found in recipient mice transplanted with SM/C-2.6-positive cells. Thus, ES-derived satellite-like cells effectively engrafted and provided long-term stem cells, which played an important role in maintenance of the integrity of the surrounding muscle tissue.

ES-derived satellite-like cells can be secondarily transplanted

For a more thorough characterization of the ES-derived satellite-like cells, we performed serial transplantations. Eight weeks after the primary cell transplantation with 2×10^4 SM/C-2.6-positive cells, the LTA muscles of the primary recipient mice were dissected to isolate the engrafted ES-derived cells, 2765 ± 685.9 (n=2; **Fig. 6*A***). The GFP^+/SM/C-2.6-positive cells within the engrafted cells were sorted by FACS (204±33.9; n=2), and only 200 GFP+/SM/C-2.6-positive cells/mouse were transplanted into predamaged LTA muscles of mdx mice (Fig. 6*B*). Eight weeks later (16 wk after the primary transplantation), the recipient mice were analyzed. GFP-positive tissue in the LTA muscle of the secondary recipient mice was observed (Fig. 6*A*). The GFP-positive tissues were confirmed to be MHC-positive mature skeletal muscle (Fig. 6*C*), and surrounding these engrafted GFP-positive skeletal muscle fascicles, dystrophin was observed (Supplemental Fig. 11). GFP/Pax7-double-positive cells located beneath the basal lamina were also detected in the engrafted tissue (Fig. 6*D*). Thus, with only 200 GFP^+SMC/2.6-positive cells, injured skeletal muscle and Pax7+ cells were successfully restored in the secondary recipients. These findings demonstrate that stem cell fraction contained within SM/C-2.6-positive cells was enriched *in vivo* through transplantation.

DISCUSSION

Many attempts have been made to induce mES cells into the skeletal muscle lineage, with hanging drop cultures for EB formation being the most widely applied method (25). However, although EBs contain cells derived from all 3 germ layers, effective induction of mES cells into the myogenic lineage, including myogenic stem cells (satellite cells), has not yet been achieved. Because of the lack of adequate surface markers, purifying ES-derived myogenic precursor/stem cells from differentiated mES cells *in vitro* has been difficult. To overcome these problems, we modified the classic EB culture system by combining it with aspects of the single-fiber culture method. Single-fiber culture (33) has been used for functional evaluation of satellite cells. When a single myofiber is plated on a Matrigel-coated plate with DMEM containing HS, satellite cells migrate out of the fiber and differentiate into myoblasts to form myofibers *in vitro*. Matrigel allows the migrating satellite cells to proliferate before differentiating and fusing into large multinucleated myotubes (35). We hypothesized that this Matrigel environment might be suitable for ES cell differentiation into satellite cells and myoblasts. Therefore, we introduced Matrigel and HS into the classic EB culture system and established an efficient induction system for myogenic lineage cells, including cells expressing Pax7, a commonly recognized marker for skeletal muscle stem cells. Furthermore, we also successfully enriched ES-derived Pax7-positive myogenic precursor/stem cells using the SM/C-2.6 antibody.

The steps in ES cell induction are thought to be homologous to normal embryogenesis. During normal skeletal myogenesis, the initial wave of myogenic precursor cells in the dermomyotome express Myf5/MRF4 and Pax3, followed by a wave of Pax3/Pax7 expression (36). These waves of myogenesis act upstream of the primary myogenic transcription factor MyoD (37-39). In myotome formation skeletal myogenesis begins with myoblasts, termed somitic myoblasts, which appear at approximately E8.5, followed by the appearance of embryonic myoblasts (E11.5), fetal myoblasts (E16.5), and, ultimately, satellite cells, which are responsible for postnatal muscle regeneration (40). Our RT-PCR results (Fig. 1*J*) showed an earlier appearance of Pax3 expression, on d 3 + 3, followed by Pax3/Pax7 expression on d 3 + 3 + 7 and stronger expression of Pax3 than Pax7. These results resemble normal myogenesis, in which the primary wave of myogenesis is followed by a secondary wave of Pax3/Pax7-dependent myogenesis (41). Considering that in the time course of myogenesis satellite cells emerge during late fetal development, ES-derived Pax7-positive cells were collected on d 3 + 3 + 14 in an attempt to acquire cells that correspond to those of the late fetal to neonatal period. However, RT-PCR results of myogenic factors in SM/C-2.6-positive cells (Fig. 2*B*) indicated that these ES-derived SM/C-2.6-positive cells are a heterogeneous population, because they express not only Pax3 and Pax7 but also Myf5 and c-met. Although further confirmation is needed, we hypothesize that both embryonic/fetal myoblasts expressing Myf-5 and/or c-met and satellite/long-term stem cells expressing Pax3/Pax7 are present.

To confirm that the ES-derived SM/C-2.6-positive cell population contained functional satellite cells, the muscle regeneration and self-renewal capacities were examined. Recently Collins *et al.* established an excellent system in which sequential damage to the muscle of a recipient mouse was applied, to evaluate both muscle regeneration and self-renewal (14) Using their experimental approach, a significant increase in numbers of both ES-derived GFP-positive muscle fascicles and GFP/Pax7-double-positive cells was observed in mice that received a second injury. This result not only demonstrates the myogenic ability of ES-derived cells but also strongly supports the idea that these cells undergo self-renewal *in vivo*.

Analysis of long-term engraftment is an important method to verify self-renewal ability, for 2 reasons. First, ES-derived satellite cells must be able to engraft for long periods of time in order to provide the amount of progeny needed for repairing damaged tissue for an

extended period. In our study the ES-derived GFP-positive skeletal muscle tissues and Pax7-positive cells engrafted up to 24 wk and were located beneath the basal lamina, which is consistent with the anatomical definition of satellite cells. Although the number of GFP-positive fascicles at 24 wk decreased compared to 12 wk, this diminution may be due to the heterogeneity of ES-derived SM/C-2.6-positive cells as we mentioned. Because myoblasts cannot support myogenesis in the long term, we believe that GFP-positive fascicles at 24 wk are products of ES-derived satellite-like cells. Second, one of the potential risks of ES cell transplantation is teratoma formation. Considering clinical applications, it is extremely important to prevent formation of teratomas in the recipients. In our study more than 60 transplanted mice were evaluated through gross morphological and histological examination. There were no teratomas formed in mice that received SM/C-2.6-positive cells, and only 1 teratoma was found among the mice that received SM/C-2.6-negative cells. This result suggests that the risk of tumor formation by the ES cells was eliminated by using sorted SM/C-2.6-positive cells.

In addition to the sequential damage model and the long-term engraftment evaluation, we performed serial transplantations to further confirm the stem cell properties of these ES-derived SM/C-2.6-positive cells. Serial transplantation enables the identification and separation of long-term stem cells from short-term progenitors (42). To eliminate myoblast involvement, we designed a serial transplantation protocol of 8 + 8 wk (*i.e.*, a second transplantation 8 wk after the primary transplantation and an analysis of recipient mice 8 wk after the second transplantation). Strikingly these recollected ES-derived SM/C-2.6-positive cells showed significantly higher engraftment efficiency compared to the primary transplantation. In the previous reports engraftment efficiencies of myoblasts transplantation was ~0.1-0.2%, with the highest reported value being 2% (43-45). This engraftment efficiency is similar to our primary transplantation (0.2-0.8%) as well as the plating efficiency of SM/C-2.6-positive cells *in vitro* (0.07%). In our study as few as 200 recollected ES-derived SM/C-2.6-positive cells were transplanted in the second transplantation, and 29.0 ± 0.47 (n=2) fascicles were observed, which indicates 14.7% of higher engraftment efficiency. Thus, through the serial transplantation, ES-derived stem cell fraction was purified. A comparison of these SM/C-2.6-positive cells before and after injection might help to characterize the stem cell fraction derived from ES cells.

There have been few reports describing transplantation of ES-derived myogenic cells into injured muscles, and the report of engraftable skeletal myoblasts derived from human ES cells represents significant progress (26). Recently Darabi *et al.* (46) have reported that by introducing Pax3 into mouse embryoid bodies, autonomous myogenesis was initiated *in vitro,* and Pax3-induced cells regenerated skeletal muscles *in vivo* by sorting the PDGF-a+Flk-1- cells. The Pax3 expression was not observed until 7 d of differentiation culture, but introduced Pax3 expression pushed EBs to myogenic differentiation. Interestingly, we observed Pax3 expression at d 3 + 3 weakly and d 3 + 3 + 7 strongly, and gene expression process in our culture is very similar to theirs. In prolonged culture using Matrigel and HS, EBs were able to initiate myogenesis without gene modification in our system.

In conclusion, we successfully generated transplantable myogenic cells, including satellite-like cells, from mES cells. The ES-derived myogenic precursor/stem cells could be enriched using a novel antibody, SM/C-2.6. These ES-derived SM/C-2.6-positive cells possess a high myogenic potential, participate in muscle regeneration, and are located beneath the basal lamina where satellite cells normally reside. The self-renewal of these ES-derived satellite-like cells enabled them to survive long-term engraftment, up to 24 wk. Through serial transplantation, these ES-derived SM/C-2.6-positive cells were further enriched and produced a high engraftment efficiency of 14.7%.

Our success in inducing mES cells to form functional muscle stem cells, the satellite-like cells, will provide an important foundation for clinical applications in the treatment of DMD patients. FJ

This work was supported by a Grant-in-Aid for Scientific Research (S) (19109006) and a Grant-in-Aid for Scientific Research (B) (18390298) from the Ministry of Education, Science, Technology, Sports, and Culture of Japan.

REFERENCES

1. Nawrotzki, R., Blake, D. J., and Davies, K. E. (1996) The genetic basis of neuromuscular disorders. *Trends Genet.* **12,** 294–298
2. Emery, A. E. (2002) The muscular dystrophies. *Lancet* **359,** 687–695
3. Michalak, M., and Opas, M. (1997) Functions of dystrophin and dystrophin associated proteins. *Curr. Opin. Neurol.* **10,** 436–442
4. Suzuki, A., Yoshida, M., Hayashi, K., Mizuno, Y., Hagiwara, Y., and Ozawa, E. (1994) Molecular organization at the glycoprotein-complex-binding site of dystrophin. Three dystrophin-associated proteins bind directly to the carboxy-terminal portion of dystrophin. *Eur. J. Biochem./FEBS* **220,** 283–292
5. Bonilla, E., Samitt, C. E., Miranda, A. F., Hays, A. P., Salviati, G., DiMauro, S., Kunkel, L. M., Hoffman, E. P., and Rowland, L. P. (1988) Duchenne muscular dystrophy: deficiency of dystrophin at the muscle cell surface. *Cell* **54,** 447–452
6. Mauro, A. (1961) Satellite cell of skeletal muscle fibers. *J. Biophys. Biochem. Cytol.* **9,** 493–495
7. Moss, F. P., and Leblond, C. P. (1971) Satellite cells as the source of nuclei in muscles of growing rats. *Anat. Rec.* **170,** 421–435
8. Snow, M. H. (1978) An autoradiographic study of satellite cell differentiation into regenerating myotubes following transplantation of muscles in young rats. *Cell Tissue Res.* **186,** 535–540
9. Jejurikar, S. S., and Kuzon, W. M., Jr. (2003) Satellite cell depletion in degenerative skeletal muscle. *Apoptosis* **8,** 573–578
10. Schultz, E., and Jaryszak, D. L. (1985) Effects of skeletal muscle regeneration on the proliferation potential of satellite cells. *Mech. Ageing Dev.* **30,** 63–72
11. Webster, C., and Blau, H. M. (1990) Accelerated age-related decline in replicative life-span of Duchenne muscular dystrophy myoblasts: implications for cell and gene therapy. *Somat. Cell Mol. Genet.* **16,** 557–565
12. Hashimoto, N., Murase, T., Kondo, S., Okuda, A., and Inagawa-Ogashiwa, M. (2004) Muscle reconstitution by muscle satellite

cell descendants with stem cell-like properties. *Development (Camb.)* **131,** 5481–5490
13. Montarras, D., Morgan, J., Collins, C., Relaix, F., Zaffran, S., Cumano, A., Partridge, T., and Buckingham, M. (2005) Direct isolation of satellite cells for skeletal muscle regeneration. *Science* **309,** 2064–2067
14. Collins, C. A., Olsen, I., Zammit, P. S., Heslop, L., Petrie, A., Partridge, T. A., and Morgan, J. E. (2005) Stem cell function, self-renewal, and behavioral heterogeneity of cells from the adult muscle satellite cell niche. *Cell* **122,** 289–301
15. Partridge, T. A., Morgan, J. E., Coulton, G. R., Hoffman, E. P., and Kunkel, L. M. (1989) Conversion of mdx myofibres from dystrophin-negative to -positive by injection of normal myoblasts. *Nature* **337,** 176–179
16. Mendell, J. R., Kissel, J. T., Amato, A. A., King, W., Signore, L., Prior, T. W., Sahenk, Z., Benson, S., McAndrew, P. E., Rice, R., Nagaraja, H., Stephens, R., Lantry, L., Morris, G. E., and Burghes, A. H. M. (1995) Myoblast transfer in the treatment of Duchenne's muscular dystrophy. *N. Engl. J. Med.* **333,** 832–838
17. Weissman, I. L., Anderson, D. J., and Gage, F. (2001) Stem and progenitor cells: origins, phenotypes, lineage commitments, and transdifferentiations. *Annu. Rev. Cell Dev. Biol.* **17,** 387–403
18. Relaix, F., Montarras, D., Zaffran, S., Gayraud-Morel, B., Rocancourt, D., Tajbakhsh, S., Mansouri, A., Cumano, A., and Buckingham, M. (2006) Pax3 and Pax7 have distinct and overlapping functions in adult muscle progenitor cells. *J. Cell Biol.* **172,** 91–102
19. Seale, P., Sabourin, L. A., Girgis-Gabardo, A., Mansouri, A., Gruss, P., and Rudnicki, M. A. (2000) Pax7 is required for the specification of myogenic satellite cells. *Cell* **102,** 777–786
20. Cornelison, D. D., and Wold, B. J. (1997) Single-cell analysis of regulatory gene expression in quiescent and activated mouse skeletal muscle satellite cells. *Dev. Biol.* **191,** 270–283
21. Hollnagel, A., Grund, C., Franke, W. W., and Arnold, H. H. (2002) The cell adhesion molecule M-cadherin is not essential for muscle development and regeneration. *Mol. Cell. Biol.* **22,** 4760–4770
22. Bottaro, D. P., Rubin, J. S., Faletto, D. L., Chan, A. M., Kmiecik, T. E., Vande Woude, G. F., and Aaronson, S. A. (1991) Identification of the hepatocyte growth factor receptor as the c-met proto-oncogene product. *Science* **251,** 802–804
23. Fukada, S., Higuchi, S., Segawa, M., Koda, K., Yamamoto, Y., Tsujikawa, K., Kohama, Y., Uezumi, A., Imamura, M., Miyagoe-Suzuki, Y., Takeda, S., and Yamamoto, H. (2004) Purification and cell-surface marker characterization of quiescent satellite cells from murine skeletal muscle by a novel monoclonal antibody. *Exp. Cell Res.* **296,** 245–255
24. Dekel, I., Magal, Y., Pearson-White, S., Emerson, C. P., and Shani, M. (1992) Conditional conversion of ES cells to skeletal muscle by an exogenous MyoD1 gene. *New Biol.* **4,** 217–224
25. Rohwedel, J., Maltsev, V., Bober, E., Arnold, H. H., Hescheler, J., and Wobus, A. M. (1994) Muscle cell differentiation of embryonic stem cells reflects myogenesis in vivo: developmentally regulated expression of myogenic determination genes and functional expression of ionic currents. *Dev. Biol.* **164,** 87–101
26. Barberi, T., Bradbury, M., Dincer, Z., Panagiotakos, G., Socci, N. D., and Studer, L. (2007) Derivation of engraftable skeletal myoblasts from human embryonic stem cells. *Nat. Med.* **13,** 642–648
27. Doetschman, T. C., Eistetter, H., Katz, M., Schmidt, W., and Kemler, R. (1985) The in vitro development of blastocyst-derived embryonic stem cell lines: formation of visceral yolk sac, blood islands and myocardium. *J. Embryol. Exp. Morphol.* **87,** 27–45
28. Niwa, H., Yamamura, K., and Miyazaki, J. (1991) Efficient selection for high-expression transfectants with a novel eukaryotic vector. *Gene* **108,** 193–199
29. Yoshimoto, M., Chang, H., Shiota, M., Kobayashi, H., Umeda, K., Kawakami, A., Heike, T., and Nakahata, T. (2005) Two different roles of purified CD45+c-Kit+Sca-1+Lin-cells after transplantation in muscles. *Stem Cells (Dayton)* **23,** 610–618
30. Harris, J. B. (2003) Myotoxic phospholipases A2 and the regeneration of skeletal muscles. *Toxicon* **42,** 933–945
31. Fukada, S., Miyagoe-Suzuki, Y., Tsukihara, H., Yuasa, K., Higuchi, S., Ono, S., Tsujikawa, K., Takeda, S., and Yamamoto, H. (2002) Muscle regeneration by reconstitution with bone marrow or fetal liver cells from green fluorescent protein-gene transgenic mice. *J. Cell Sci.* **115,** 1285–1293
32. Gross, J. G., and Morgan, J. E. (1999) Muscle precursor cells injected into irradiated mdx mouse muscle persist after serial injury. *Muscle Nerve* **22,** 174–185
33. Rosenblatt, J. D., Lunt, A. I., Parry, D. J., and Partridge, T. A. (1995) Culturing satellite cells from living single muscle fiber explants. *In Vitro Cell. Dev. Biol.* **31,** 773–779
34. Dhawan, J., and Rando, T. A. (2005) Stem cells in postnatal myogenesis: molecular mechanisms of satellite cell quiescence, activation and replenishment. *Trends Cell Biol.* **15,** 666–673
35. Zammit, P. S., Relaix, F., Nagata, Y., Ruiz, A. P., Collins, C. A., Partridge, T. A., and Beauchamp, J. R. (2006) Pax7 and myogenic progression in skeletal muscle satellite cells. *J. Cell Sci.* **119,** 1824–1832
36. Relaix, F., Rocancourt, D., Mansouri, A., and Buckingham, M. (2005) A Pax3/Pax7-dependent population of skeletal muscle progenitor cells. *Nature* **435,** 948–953
37. Tajbakhsh, S., Rocancourt, D., Cossu, G., and Buckingham, M. (1997) Redefining the genetic hierarchies controlling skeletal myogenesis: Pax-3 and Myf-5 act upstream of MyoD. *Cell* **89,** 127–138
38. Kiefer, J. C., and Hauschka, S. D. (2001) Myf-5 is transiently expressed in nonmuscle mesoderm and exhibits dynamic regional changes within the presegmented mesoderm and somites I-IV. *Dev. Biol.* **232,** 77–90
39. Hirsinger, E., Malapert, P., Dubrulle, J., Delfini, M. C., Duprez, D., Henrique, D., Ish-Horowicz, D., and Pourquie, O. (2001) Notch signalling acts in postmitotic avian myogenic cells to control MyoD activation. *Development (Camb.)* **128,** 107–116
40. Smith, T. H., Block, N. E., Rhodes, S. J., Konieczny, S. F., and Miller, J. B. (1993) A unique pattern of expression of the four muscle regulatory factor proteins distinguishes somitic from embryonic, fetal and newborn mouse myogenic cells. *Development (Camb.)* **117,** 1125–1133
41. Kassar-Duchossoy, L., Giacone, E., Gayraud-Morel, B., Jory, A., Gomes, D., and Tajbakhsh, S. (2005) Pax3/Pax7 mark a novel population of primitive myogenic cells during development. *Genes Dev.* **19,** 1426–1431
42. Harrison, D. E., Astle, C. M., and Delaittre, J. A. (1978) Loss of proliferative capacity in immunohemopoietic stem cells caused by serial transplantation rather than aging. *J. Exp. Med.* **147,** 1526–1531
43. Yao, S. N., and Kurachi, K. (1993) Implanted myoblasts not only fuse with myofibers but also survive as muscle precursor cells. *J. Cell Sci.* **105**(Pt. 4), 957–963
44. Rando, T. A., and Blau, H. M. (1994) Primary mouse myoblast purification, characterization, and transplantation for cell-mediated gene therapy. *J. Cell Biol.* **125,** 1275–1287
45. Sherwood, R. I., Christensen, J. L., Conboy, I. M., Conboy, M. J., Rando, T. A., Weissman, I. L., and Wagers, A. J. (2004) Isolation of adult mouse myogenic progenitors: functional heterogeneity of cells within and engrafting skeletal muscle. *Cell* **119,** 543–554
46. Darabi, R., Gehlbach, K., Bachoo, R. M., Kamath, S., Osawa, M., Kamm, K. E., Kyba, M., and Perlingeiro, R. C. (2008) Functional skeletal muscle regeneration from differentiating embryonic stem cells. *Nat. Med.* **14,** 134–143

Received for publication October 21, 2008.
Accepted for publication January 8, 2009.

Biochemical and Biophysical Research Communications 387 (2009) 482–488

Contents lists available at ScienceDirect

Biochemical and Biophysical Research Communications

journal homepage: www.elsevier.com/locate/ybbrc

The effects of cardioactive drugs on cardiomyocytes derived from human induced pluripotent stem cells

Noritaka Yokoo [a], Shiro Baba [a], Shinji Kaichi [a], Akira Niwa [a], Takahiro Mima [a], Hiraku Doi [a], Shinya Yamanaka [b], Tatsutoshi Nakahata [b], Toshio Heike [a,*]

[a] Department of Pediatrics, Graduate School of Medicine, Kyoto University, 54 Kawahara-cho, Shogoin, Sakyo-ku, Kyoto 606-8507, Japan
[b] Center for iPS Cell Research and Application (CiRA), Institute for Integrated Cell-Material Sciences, Kyoto University, 53 Kawahara-cho, Shogoin, Sakyo-ku, Kyoto 606-8507, Japan

ARTICLE INFO

Article history:
Received 7 July 2009
Available online 16 July 2009

Keywords:
Human induced pluripotent stem cell
Human embryonic stem cell
Cardiomyocytes
Drug loading test
Arrhythmia

ABSTRACT

Developing effective drug therapies for arrhythmic diseases is hampered by the fact that the same drug can work well in some individuals but not in others. Human induced pluripotent stem (iPS) cells have been vetted as useful tools for drug screening. However, cardioactive drugs have not been shown to have the same effects on iPS cell-derived human cardiomyocytes as on embryonic stem (ES) cell-derived cardiomyocytes or human cardiomyocytes in a clinical setting. Here we show that current cardioactive drugs affect the beating frequency and contractility of iPS cell-derived cardiomyocytes in much the same way as they do ES cell-derived cardiomyocytes, and the results were compatible with empirical results in the clinic. Thus, human iPS cells could become an attractive tool to investigate the effects of cardioactive drugs at the individual level and to screen for individually tailored drugs against cardiac arrhythmic diseases.

Introduction

The long-QT syndrome (LQTS) is characterized by an abnormal prolongation of the QT-interval on the ECG and an increased risk of sudden death, due to ventricular fibrillation known as Torsade de Pointes (TdP) [1]. In a previous study [2], four patients died suddenly (1.3% per year) during an average follow-up period of 26 months per patient and among 196 idiopathic LQTS patients, 27 experienced one or more syncopal episodes (8.6% per year). Molecular genetic studies have revealed several forms of congenital LQTS caused by mutations in genes coding for potassium, sodium and calcium channels or membrane adapters [3–6]. Preliminary clinical studies have since suggested the feasibility of performing genotype-specific therapy with therapeutic agents that abbreviate the QT-interval [7]. But it is difficult to select the correct drug because within the same LQTS subtype, the same drug can sometimes have different effects depending on the patient.

Furthermore, the diagnosis of LQTS subtypes is difficult. Genetic testing can only identify 50–75% of probands [8]. So an epinephrine challenge is needed in some patients to diagnose LQTS in a clinical setting [9]. However, this test sometimes induces TdP, so it must be done under careful patient surveillance.

The generation of iPS cells from human fibroblast using a combination of 4 transcription factors (*Oct3/4*, *Sox2*, *Klf4*, and *c-Myc*) has opened remarkable new avenues for not only basic research but also regenerative medicine, understanding of disease mechanisms, drug screening, and toxicology [10]. A recent study reported the generation of disease-specific iPS cell lines from patients with a variety of diseases [11]. If patient-specific iPS cells could be commonly generated and employed in a clinical setting, they could become a useful tool for selecting the best drug for individual LQTS patients.

But there has been no report that cardiomyocytes derived from human iPS cells respond to drugs in the same way as human cardiomyocytes. It is important to investigate whether cardiomyocytes derived from human iPS cells react to drugs in the same way as human cardiomyocytes, if patient-specific iPS cells are to be used in a clinical setting for drug screening. Previous studies have hinted that some drugs produce the same effects in cardiomyocytes as in cardiomyocytes derived from ES cells [12–14]. In this study, we investigated whether cardiomyocytes derived human iPS cells responded to drugs in the same way as in cardiomyocytes derived from human ES cells with respect to beating frequency and contractility, and we compared these results with previously described clinical empirical results [15].

Materials and methods

Human iPS and human ES cell culture. We used human ES cell line, KhES1, and human iPS cell lines 201B7. Human iPS cells and human ES cells were maintained on mitomycin-C (Kyowa Hakkoh)

* Corresponding author. Fax: +81 75 752 2361.
E-mail address: heike@kuhp.kyoto-u.ac.jp (T. Heike).

0006-291X/$ - see front matter © 2009 Elsevier Inc. All rights reserved.
doi:10.1016/j.bbrc.2009.07.052

treated mouse embryonic fibroblasts (MEFs) or SNLs on cell culture dishes. In brief, both human iPS and human ES cells were maintained in DMEM/F12 culture medium (SIGMA) supplemented with 20% knock-out serum replacement (Gibco), 0.1 mmol/L nonessential amino acids (Gibco), 4 mmol/L L-glutamine, 0.8 μmol/L basic fibroblast growth factor (bFGF) (Invitrogen).

Embryoid body formation and cardiac differentiation. Colonies were detached from cell culture dishes by incubating them with PBS containing 0.25% trypsin (Gibco) and 1 mg/mL collagenase I (Worthington) at 37 °C for 3–4 min. The cells were then placed in petri dishes (Sterilin) in suspension cultures for 7 days with maintenance medium supplemented with 5 ng/ml bFGF. Embryoid bodies (EBs) were then plated on 0.1% gelatin-coated 6-well culture plates (BD Biosciences) and cultured in cardiac differentiation medium, consisting of alpha MEM (Gibco) supplemented with 0.5 μmol/L 2ME and 10% FCS (Hyclone) (changed once every 7 days). Contractile colonies appeared 15–25 days after plating on gelatin-coated dishes (Fig. 1A).

Reverse transcriptase polymerase chain reaction (RT-PCR). Total RNA was isolated using TRIzol Reagent (Invitrogen) from undifferentiated iPS cells, EBs derived from human iPS cells, the contracting areas of differentiated human iPS cells, and human right ventricular tissue (obtained by a tetralogy of Fallot patient that had received a right flow ventricular tract ventriculotomy). Total RNA was used for oligo (dT) 12–18-primed reverse transcription using the Super Script II First-Strand Synthesis System (Invitrogen). RT-PCR was carried out using Ex Taq (TAKARA BIO). PCR conditions included denaturation at 94 °C for 30 s, annealing at 60 °C for 30 s, and extension at 55–65 °C for 1 min for 25–35 cycles, with a final extension at 72 °C for 7 min. Primers used are listed in Table 3.

Immunohistochemistry. Contractile colonies were partitioned into small particles using collagenase I (Worthington) for 2 h at 37 °C. The cells were then washed and plated on 6-well culture plates coated with 0.1% gelatin for 2 or 3 days to allow attachment. Cells were fixed in 4% paraformaldehyde for 15 min at 4 °C. Then the cells were incubated with primary antibodies, such as polyclonal anti-cardiac Troponin I (IgG, 1:50 dilution; Santa Cruz Biotechnology), polyclonal anti-MLC2v (IgG, 1:50 dilution; Santa Cruz Biotechnology), or polyclonal anti-ANP (IgG, 1:250 dilution; Chemicon) in 2% skim milk with 0.1% Triton X-100 overnight at 4 °C. Secondary antibodies were cyanine 3 (Cy3)-conjugated donkey anti-rat IgG (1:200 dilution; Jackson Immunoresearch), Cy3-conjugated donkey anti-rabbit IgG (1:200 dilution; Jackson Immunoresearch), and Cy3-conjugated donkey anti-goat IgG (1:200 dilution; Jackson Immunoresearch). Nuclei were counter-stained with Hoechst 33342 (Molecular probes).

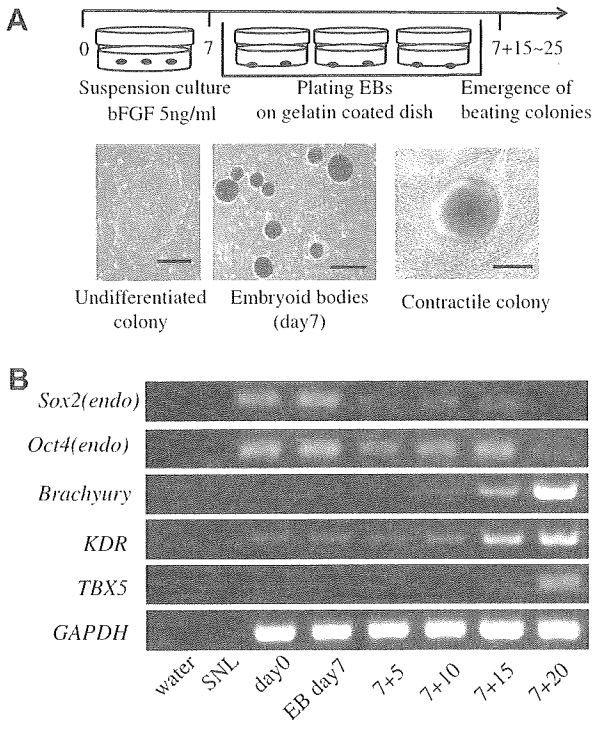

Fig. 1. An outline of the protocol used for the differentiation of human iPS cells and human ES cells. Scale bars = 200 μm (A). Time course analysis of immature gene expression, mesodermal markers, and cardiac progenitor markers during differentiation (B).

Electrophysiological examination. Microelectrode arrays analysis was performed to investigate the electrophysiological potential of cardiomyocytes derived from human iPS cells using the MED 64 system (Alpha MED Sciences) [16–18]. Micro-dissected contracting areas were plated on MED-probe dishes (Alpha MED Sciences) followed by incubation for 3–7 days to allow attachment. The potentials of the contractile colonies derived from these cells were then recorded.

Drug loading test. Differentiation medium was replaced with alpha MEM containing 10 mmol/L HEPES buffer (Nacalai tesque), 7 mol/L NaCl, and 0.5 μmol/L 2ME, which was adjusted to pH 7.4 with NaOH. After 10 min incubation at 37 °C, the frequency and contractility of the contractile colonies were measured in a movie recorded by a VB 7000 (KEYENCE) camera under drug-free medium conditions as well as under drug conditions with three different drug concentrations. Beating colonies were selected when the beating rate was 40/min to 60/min under drug-free medium conditions. Colonies whose contractile motion was distended were excluded. Loading drugs were as follows; isoproterenol (SIGMA), adrenaline (Dai-ichi Sankyo), propranolol (SIGMA), procainamide (Dai-ichi Sankyo), mexiletine (Boehringer Ingelheim), flecainide (Eisai), verapamil (SIGMA), and amiodarone (Sanofi-aventis).

Analysis of beating rate and contractility. Beating rates were counted based on the video recordings. Recently, some papers reported that video-edge detecting systems are useful for calculating the contractility of contractile colonies [12]. We imitated this method and calculated the contractility of colonies. In brief, we extracted the still images of systolic phase and diastolic phase from the recorded video images. The major axis of each phase was measured and the contractile index was defined as $a - b/a$ (a: length of diastolic phase, b: the length of systolic phase) (Fig. 4A).

Statistics. Data are presented as means ± SEM. Statistical significance was determined by the unpaired t-test for two samples and one-way ANOVA followed by the Scheffe test for more than three samples. P values <0.05 were considered to be statistically significant.

Results

Time course analysis of gene expression during cardiac differentiation

First, we examined the time course of gene expression during cardiac differentiation of human iPS cells by RT-PCR to compare it with that of normal embryogenesis (Fig. 1B). Undifferentiated human iPS cells strongly expressed endogenous *Oct4* and *Sox2*, which are undifferentiated cell markers, but did not express the mesodermal marker *Brachyury* or the cardiac progenitor marker *TBX5* (Fig. 1B). *KDR* was weakly expressed. These results show that undifferentiated human iPS cells have similar properties to undifferentiated human ES cells [19]. Endogenous *Oct4* and *Sox2* expression gradually decreased during culture in differentiation medium. The

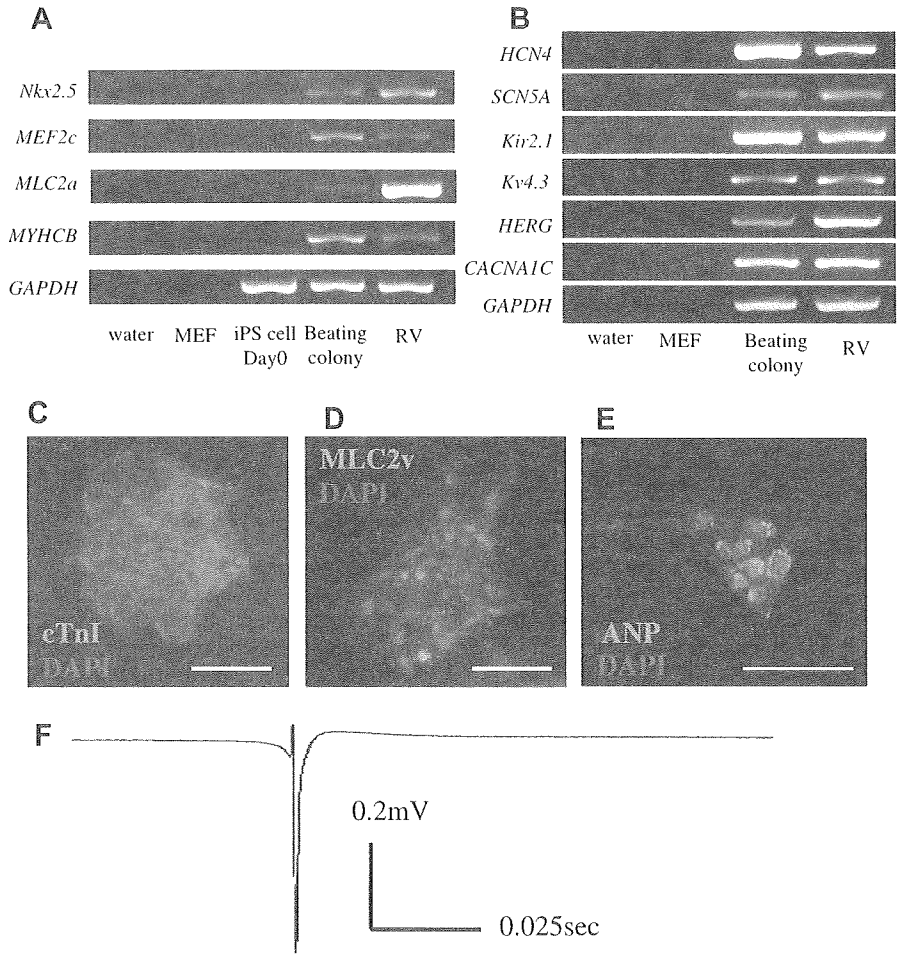

Fig. 2. Gene expression analyses of cardiac markers by RT-PCR (A). Gene expression analysis of ion channel related genes (B). Immunohistochemistry of contractile colonies. Colonies were stained with cTnI (C), MLC2v (D), or ANP (E). Scale bars = 100 μm. Field potentials of contractile colonies measured by the MED 64 system (F).

expression of the mesodermal marker *Brachyury* increased from day 10 after EB formation. The expression of *KDR* also gradually increased from day 10 after EB formation. These patterns of mesodermal marker expression are compatible with those of human ES cells as previously described [19]. The cardiac progenitor marker *TBX5* was expressed from day 20 after EB formation, which is compatible with the gene expression patterns seen during cardiac formation in embryogenesis and human ES cell differentiation as previously described [19]. The result additionally suggests that human iPS cells differentiated into the mesodermal lineage and then differentiated into contractile colonies via cardiac progenitor cells.

Cardiac differentiation of human iPS cells via EBs

Next, we examined the contractile colonies consisting of cardiac-specific cells. Contractile colonies were observed from 15 to 25 days after EB formation both in human iPS and human ES cell populations. This result demonstrates that our differentiation methods could generate contractile colonies from both human iPS cells and human ES cells. Next, we investigated whether these contractile colonies were human cardiomyocytes. For this purpose, we carried out RT-PCR and examined for the expression of cardiac cell markers. RT-PCR showed that contractile colonies expressed cardiac markers *Nkx2.5*, *MEF2c*, *MLC2a*, and *MYHCB* (Fig. 2A). Moreover, we carried out immunohistochemical analysis to confirm that the contractile colonies were human cardiomyocytes. Contractile colonies were stained by the cardiac cell marker, cTnI, the ventricular cell marker, MLC2v, and the atrial cell marker, ANP. The colonies were also stained by cTnI, and some of them were stained by MLC2v or ANP (Fig. 2C–E). These results of immunohistochemical analysis confirmed that the contractile colonies were indeed human cardiomyocytes.

Electrical analysis of contractile colonies

To investigate whether the contractile colonies that expressed cardiac markers were electrically functional cardiac colonies, we measured their electrical potentials by microelectrode array analysis using the MED 64 system (Alpha MED Sciences) [16–18]. The field potentials of the contractile colonies were comparable to those of cardiomyocytes derived from human ES cells as previously reported (Fig. 2F) [16–18]. Moreover, RT-PCR showed that these cells expressed the If channel (*HCN4*), the L-type calcium channel (*CACNA1C*), the sodium channel (*SCN5A*), the inward rectifier (*Kir2.1*), the transient outward channel (*Kv4.3*), and the delayed rectifier IKr (*HERG*) (Fig. 2B).

Effects of drugs on the beating frequency of cardiomyocytes derived from human iPS cells

We next investigated whether the cardiomyocytes derived from iPS cells reacted with cardioactive drugs in the same manner as

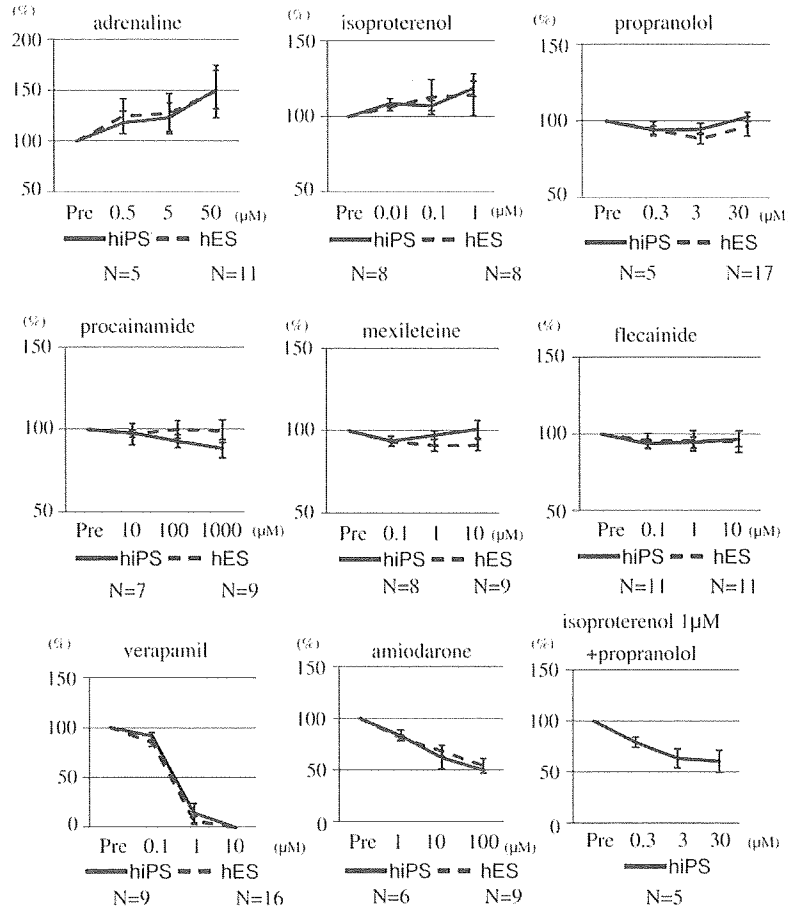

Fig. 3. The effects of cardioactive drugs on the beating rates of contractile colonies derived from human iPS cells and human ES cells. Adrenaline, isoproterenol, verapamil, amiodarone, and isoproterenol + propranolol had statistically significant effects between pre-drug loading and the maximum concentration of the drug used in cardiomyocytes derived from human iPS cells ($P < 0.05$). There were no statistically significant differences between the concentrations of drugs that elicited effects in human iPS cells and those that elicited effects in human ES cells.

cardiomyocytes derived from human ES cells by performing drug loading tests. First we compared the beating frequencies of these two cell populations. A total of eight drugs were tested (see Table 1 for the list of drugs and their concentrations). The β stimulants, adrenaline and isoproterenol increased beating frequency in a dose dependent manner. The β blocker, propranolol, and the Na channel blockers, procainamide, mexiletine, and flecainide had no effect on beating frequency. The Ca channel blocker verapamil decreased beating frequency in a dose dependent manner, and all contractile colonies ceased to contract when 1×10^{-5} M verapamil was loaded. Amiodarone, which mainly acts as a K channel blocker, decreased beating frequency in a dose dependent manner. We carried out β blocker loading in the presence of 1×10^{-6} M isoproterenol in order to mimic conditions *in vivo* [20]. Under this condition, the beating frequency decreased in a dose dependent manner. There were no statistical differences between the drug concentrations required to elicit the effects in human iPS cells and those required to elicit the effects in cardiomyocytes derived from human ES cells (Fig. 3). Previous reports showed that some drugs had similar effects on the beating frequency of cardiomyocytes derived from ES cells and on *bone-fide* human cardiomyocytes, suggesting that human iPS cells and cardiomyocytes respond similarly to these drugs as well [12–14]. Table 2 shows a comparison of the effects of drug loading on human iPS cells and the effects of these drugs in a clinical setting [15]. As the effects are broadly similar and occur within the same range of drug concentrations, we conclude that cardiomyocytes derived from human iPS cells are a good model for testing the effects of drugs on the beating frequency of human cardiomyocytes. The results are also compatible with previously reported clinical empirical results [15].

The effects of drugs on the contractility of cardiomyocytes derived from human iPS cells

Next, we investigated the effects of drugs on the contractility of human iPS cells and cardiomyocytes derived from human ES cells. The results showed that adrenaline and isoproterenol increased contractility in a dose dependent manner. Propranolol, mexiletine, or amiodarone had no effect on contractility. Verapamil decreased contractility in a dose dependent manner, and all contractile colonies ceased to contract when 1×10^{-5} M verapamil was loaded. Procainamide and flecainide also decreased the beating frequency in a dose dependent manner. We also carried out β blocker loading in the presence of 1×10^{-6} M isoproterenol with cardiomyocytes derived from human iPS cells, which showed that contractility again decreased in a dose dependent manner under these conditions. There were no statistical differences between the drug concentrations required to elicit the effects in human iPS cells and those required to elicit the effects in cardiomyocytes derived from human ES cells (Fig. 4B). Previous reports have shown that some

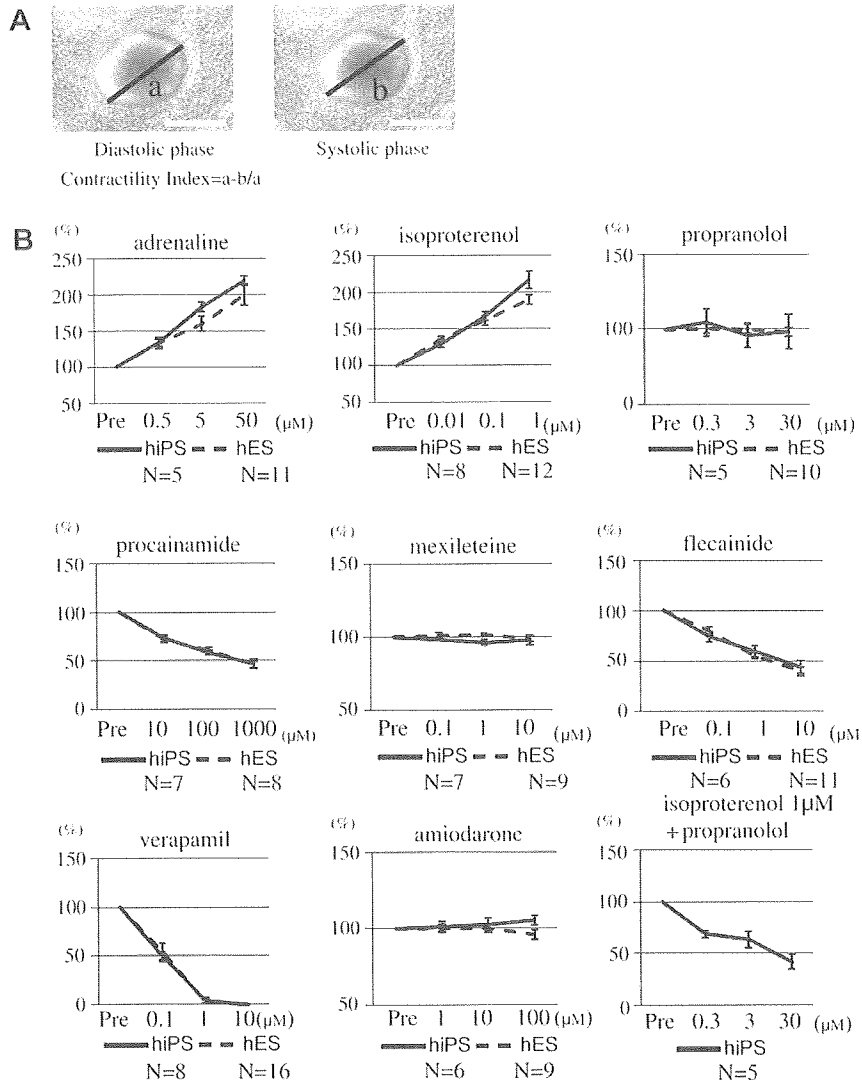

Fig. 4. Calculation of the contractility index. Right panel; diastolic phase, left panel; systolic phase. Scale bars = 200 μm (A). The effects of cardioactive drugs on the contractility of contractile colonies derived from human iPS cells and human ES cells. Adrenaline, isoproterenol, procainamide, flecainide, verapamil, and isoproterenol + propranolol had statistically significant effects on human iPS cells between pre-drug loading and the maximum concentration of the drug used in cardiomyocytes derived from human iPS cells ($P < 0.05$). There were no statistically significant differences between the concentrations of drugs that elicited effects in human iPS cells and those that elicited effects in human ES cells (B).

drugs had similar effects on the beating frequency of cardiomyocytes derived from ES cells and on *bone-fide* human cardiomyocytes, suggesting that human iPS cells and cardiomyocytes respond similarly to these drugs as well [12]. The results were compatible with clinical empirical results [15]. So we conclude that cardiomyocytes derived from human iPS cells respond similarly to drugs that affect contractility in human cardiomyocytes.

Table 1
Drugs and concentrations.

Class	Drugs	Concentration (M)
Na channel blocker	Procainamide	1×10^{-5}–1×10^{-3}
	Mexiletine	1×10^{-7}–1×10^{-5}
	Flecainide	1×10^{-7}–1×10^{-5}
β blocker	Propranolol	3×10^{-7}–3×10^{-5}
K channel blocker	Amiodarone	1×10^{-6}–1×10^{-4}
Ca channel blocker	Verapamil	1×10^{-7}–1×10^{-5}
α, β stimulant	Adrenaline	5×10^{-7}–5×10^{-5}
β stimulant	Isoproterenol	1×10^{-8}–1×10^{-6}

Table 2
Comparison with clinical empirical result.

Drugs	Result		Clinical efficacy	
	Contractility	Beating frequency	Contractility	Beating frequency
Procainamide	↓	→	↓	→
Mexiletine	→	→	→	→
Flecainide	↓	→	↓	→
Propranolol	↓	↓	↓	↓
Amiodarone	→	↓	→	↓
Verapamil	↓	↓	↓	↓
Isoproterenol	↑	↑	↑	↑
Adrenaline	↑	↑	↑	↑

Table 3
Primers for RT-PCR.

Genes	Direction	Sequence
Oct4 (endo)	Forward	GACAGGGGGAGGGGAGGAGCTAGG
	Reverse	CITCCCTCCAACCAGTTGCCCCAAAC
Sox2 (endo)	Forward	GGGAAATGGGAGGGGTGCAAAAGAGG
	Reverse	TTGCGTGAGTGTGGATGGGATTGGTG
C-KIT	Forward	ATTCCCAGCCCATGAGTCCTTGA
	Reverse	ACACGTGGAACACCAACATCCT
Brachyury	Forward	AAGGTGGATCTTCAGGTAGC
	Reverse	CATCTCATTGGTGAGCTCC
KDR	Forward	AAAACCTTTTGTTGCTTTTGG
	Reverse	GAAATGGGATTGGTAAGGATG
Nkx2.5	Forward	GCGATTATGCAGCGTGCAATGAGT
	Reverse	AACATAAATACGGGTGGGTGCGTG
TBX5	Forward	AAATGAAACCCAGCATAGGAGCTGGC
	Reverse	ACACTCAGCCTCACATCTTACCCT
MEF2c	Forward	TTTAACACCGCCAGCGCTCTTCACCTTG
	Reverse	TCGTGGCGCGTGTGTTGTGGGTATCTCG
MLC2a	Forward	ACATCATCACCCACGGAGAAGAGA
	Reverse	ATTGGAACATGGCCTCTGGATGGA
MYHCB	Forward	CTGGAGGCCGAGCAGAAGCGCAACG
	Reverse	GTCCGCCCGCTCCTCTGCCTCATCC
HCN4	Forward	GGTGTCCATCAACAACATGG
	Reverse	TGTACTGCTCCACCTGCTTG
SCN5A	Forward	CCTAATCATCTTCCGCATCC
	Reverse	TGTTCATCTCTCTGTCCTCATC
Kir2.1	Forward	GACCTGGAGACGGACGAC
	Reverse	AGCCTGGAGTCTGTCAAAGTC
Kv4.3	Forward	GCCAGTCCCTGTGATTGTTT
	Reverse	CTCCATGCAGTTCTGCTCAA
HERG	Forward	TCCAGCGGCTGTACTCGGGC
	Reverse	TGGACCAGAAGTGGTCGGAGAACTC
CACNA1C	Forward	AACATCAACAACGCCAACAA
	Reverse	AGGGCAGGACTGTCTTCTGA
GAPDH	Forward	CACCAGGGCGCTTTTAACTCTG
	Reverse	ATGGTTCACACCCATGCGAAC

Discussion

In this report, we differentiated human iPS cells into cardiomyocytes, and compared the effects of drugs on cardiomyocytes derived from these cells and on cardiomyocytes derived from human ES cells, as well as with empirical results obtained in a clinical setting. The time course analysis of gene expression during cardiac differentiation was compatible to that seen during cardiogenesis of normal embryogenesis, and the results of the drug loading tests showed that cardiomyocytes derived from human iPS cells responded to drugs in much the same way as cardiomyocytes derived from human ES cells. The results were also compatible to empirical results obtained in a clinical setting.

Human iPS cells can be generated from somatic cell by introducing transcriptional factors. This technology is expected to generate patient-specific iPS cells suitable for the study of disease mechanisms, drug screening, and toxicology studies. This technology is easier to implement for the generation of patient-specific pluripotent cells than current technology which relies on nuclear transplantation technology to generate patient-specific pluripotent cells from ES cells. If cardiomyocytes derived from iPS cells could be shown to respond to drugs in the same way as human derived cardiomyocytes, then this technology would also constitute a major advance because it would allow the use of patient-specific iPS cell for the screening of patient-specific drugs against arrhythmic diseases, especially for lethal arrhythmic diseases such as LQTS where it is often very difficult to select for the best drug.

As the generation of cardiomyocytes from human iPS cells relies on the introduction of exogenous genes, we addressed the troublesome issue of whether cardiomyocytes derived from human iPS cells would respond to drugs in the same way as normal human cardiomyocytes. We considered the beating frequency and contractility to be very important indicators, because heart pump function is defined by beating frequency and contractility. So we investigated the effects of drugs on these two indicators, and found that drugs affect the beating frequency and contractility of cardiomyocytes derived from human iPS cells in much the same way as they do in a clinical setting. This result suggests that cardiomyocytes derived from human iPS cells could be used for drug screening tests instead of current screening procedures in a clinical setting. Cardiomyocytes derived from ES cells also responded to drugs in the same way as cardiomyocytes derived from human iPS cells.

Thus, these results suggest that patient-specific iPS cells could be used to select for the best drug to treat arrhythmic disease at the individual level, and would have the additional advantage of allowing the massive and rapid screening of drugs at concentrations that would be normally prohibitive in patients. However, until further studies are carried out, it is probably still too early to conclude that the drug effects on human iPS cell lines and patients are identical.

In conclusion, cardiomyocytes derived from human iPS cells have tremendous potential for drug screening, which should open the possibility of using patient-specific iPS cells in a clinical setting. The best drugs could be selected safely and rapidly by using human iPS cells from individual patients.

References

[1] A.J. Moss, J. McDonald, Unilateral cervicothoracic sympathetic ganglionectomy for the treatment of long QT interval syndrome, N. Engl. J. Med. 285 (1971) 903–904.
[2] A.J. Moss, P.J. Schwartz, R.S. Crampton, E. Locati, E. Carleen, The long QT syndrome: a prospective international study, Circulation 71 (1985) 17–21.
[3] M.C. Sanguinetti, C. Jiang, M.E. Curran, M.T. Keating, A mechanistic link between an inherited and an acquired cardiac arrhythmia: HERG encodes the IKr potassium channel, Cell 81 (1995) 299–307.
[4] Q. Wang, J. Shen, I. Splawski, D.L. Atkinson, Z.Z. Li, J.L. Robinson, A.J. Moss, J.A. Towbin, M.T. Keating, SCN5A mutations associated with an inherited cardiac arrhythmia, long QT syndrome, Cell 89 (1995) 805–811.
[5] I. Splawski, J. Shen, K.W. Timothy, M.H. Lehmann, S. Priori, J.L. Robinson, A.J. Moss, P.J. Schwartz, J.A. Towbin, G.H. Vincent, M.T. Keating, Spectrum of mutations in long-QT syndrome genes. KVLQT1, HERG, SCN5A, KCNE1, and KCNE2, Circulation 102 (2000) 1178–1185.
[6] I. Splawski, K.W. Timothy, L.M. Sharpe, N. Decher, P. Kumar, R. Bloise, C. Napolitano, P.J. Schwartz, R.M. Joseph, K. Condouris, H.T. Flusberg, S.G. Priori, M.C. Sanguinetti, M.T. Keating, Ca(V)1.2 calcium channel dysfunction causes a multisystem disorder including arrhythmia and autism, Cell 119 (2004) 19–31.
[7] P.J. Schwartz, S.G. Priori, C. Spazzolini, A.J. Moss, G.M. Vincent, C. Napolitano, I. Denjoy, P. Guicheneney, G. Breithardt, M.T. Keating, A.A. Wilde, L. Toivonen, W. Zareba, J.L. Robinson, K.W. Timothy, V. Corfield, D. Wattanasirichaigoon, C. Corbett, W. Haverkamp, E. Schulze-Bahr, M.H. Lehmann, K. Schwartz, P. Coumel, R. Bloise, Genotype–phenotype correlation in the long-QT syndrome: gene-specific triggers for life-threatening arrhythmias, Circulation 103 (2001) 89–95.
[8] D.J. Tester, L.B. Cronk, J.L. Carr, V. Schulz, B.A. Salisbury, R.S. Judson, M.J. Ackerman, Allelic dropout in long QT syndrome genetic testing: a possible mechanism underlying false-negative results, Heart Rhythm 3 (2006) 815–821.
[9] H. Vyas, J. Hejlik, M.J. Ackerman, Epinephrine QT stress testing in the evaluation of congenital long-QT syndrome: diagnostic accuracy of the paradoxical QT response, Circulation 113 (2006) 1385–1392.
[10] K. Takahashi, K. Tanabe, M. Ohnuki, M. Narita, T. Ichisaka, K. Tomoda, S. Yamanaka, Induction of pluripotent stem cells from adult human fibroblasts by defined factors, Cell 131 (2007) 861–872.
[11] I.H. Park, N. Arora, H. Huo, N. Maherali, T. Ahfeldt, A. Shimamura, M.W. Lensch, C. Cowan, K. Hochedlinger, G.Q. Dale, Disease-specific induced pluripotent stem cells, Cell 134 (2008) 877–886.
[12] J.Q. He, Y. Ma, Y. Lee, J.A. Thomson, T.J. Kamp, Human Embryonic stem cells develop into multiple types of cardiac myocytes, Circ. Res. 93 (2003) 32–39.

[13] M. Reppel, C. Boettinger, J. Hescheler, Beta-adrenergic and muscarinic modulation of human embryonic stem cell-derived cardiomyocytes, Cell. Physiol. Biochem. 14 (2004) 187–196.
[14] C. Xu, S. Polic, N. Rao, M.K. Carpenter, Characterization and enrichment of cardiomyocytes derived from human embryonic stem cells, Circ. Res. 91 (2002) 501–508.
[15] M.R. Rosen, Consequences of the Sicilian Gambit, Eur. Heart J. 16 (Suppl. G) (1995) 32–36.
[16] J. Hescheler, M. Halbach, U. Egert, H. Bohlen, B.K. Fleischmann, M. Reppel, Determination of electrical properties of ES cell-derived cardiomyocytes using MEAs, J. Electrocardiol. 37 (Suppl.) (2004) 110–116.
[17] M. Reppel, F. Pillekamp, K. Brockmeier, M. Matzkies, A. Bekcioglu, T. Lipke, F. Nquemo, H. Bonnemeier, J. Hescheler, The electrocardiogram of human embryonic stem cell derived cardiomyocytes, J. Electrocardiol. 38 (2005) 166–170.
[18] M. Reppel, P. Igelmund, U. Egert, F. Juchelka, J. Hescheler, I. Drobinskaya, Effect of cardioactive drugs on action potential generation and propagation in embryonic stem cell-derived cardiomyocytes, Cell. Physiol. Biochem. 19 (2007) 213–224.
[19] L. Yang, M.H. Soonpaa, A.D. Adler, T.K. Roepke, S.J. Kattman, M. Kennedy, M.E. Henckaerts, K. Bonham, G.W. Abbott, R.M. Linden, L.J. Field, G.M. Keller, Human cardiovascular progenitor cells develop from a KDR$^+$ embryonic-stem-cell-derived population, Nature 453 (2008) 524–528.
[20] W. Shimizu, C. Antzelevitch, Cellular basis for the ECG features of the LQT1 form of the long-QT syndrome, Circulation 98 (1998) 2314–2322.

Journal of Cellular Physiology

Orderly Hematopoietic Development of Induced Pluripotent Stem Cells via Flk-1$^+$ Hemoangiogenic Progenitors

AKIRA NIWA,[1,2] KATSUTSUGU UMEDA,[1] HSI CHANG,[1] MEGUMU SAITO,[1,2] KEISUKE OKITA,[3] KAZUTOSHI TAKAHASHI,[3] MASATO NAKAGAWA,[3,4] SHINYA YAMANAKA,[3,4] TATSUTOSHI NAKAHATA,[1,2] AND TOSHIO HEIKE[1]*

[1]*Department of Pediatrics, Graduate School of Medicine, Kyoto University, Kyoto, Japan*

[2]*Clinical Application Department, Center for iPS cell Research and Application (CiRA), Institute for Integrated Cell-Material Sciences, Kyoto University, Kyoto, Japan*

[3]*Basic Biology Department, Center for iPS cell Research and Application (CiRA), Institute for Integrated Cell-Material Sciences, Kyoto University, Kyoto, Japan*

[4]*Department of Stem Cell Biology, Institute for Frontier Medical Sciences, Kyoto University, Kyoto, Japan*

Induced pluripotent stem (iPS) cells, reprogrammed somatic cells with embryonic stem (ES) cell-like characteristics, are generated by the introduction of combinations of specific transcription factors. Little is known about the differentiation of iPS cells in vitro. Here we demonstrate that murine iPS cells produce various hematopoietic cell lineages when incubated on a layer of OP9 stromal cells. During this differentiation, iPS cells went through an intermediate stage consisting of progenitor cells that were positive for the early mesodermal marker Flk-1 and for the sequential expression of other genes that are associated with hematopoietic and endothelial development. Flk-1$^+$ cells differentiated into primitive and definitive hematopoietic cells, as well as into endothelial cells. Furthermore, Flk-1$^+$ populations contained common bilineage progenitors that could generate both hematopoietic and endothelial lineages from single cells. Our results demonstrate that iPS cell-derived cells, like ES cells, can follow a similar hematopoietic route to that seen in normal embryogenesis. This finding highlights the potential use of iPS cells in clinical areas such as regenerative medicine, disease investigation, and drug screening.
J. Cell. Physiol. 221: 367–377, 2009.

Because of their pluripotency and potential for self-renewal, embryonic stem (ES) cells have been used in various fields of science, including developmental biology (Evans and Kaufman, 1981). ES cells can differentiate into multiple cell types in a similar way to that observed in vivo. Previous studies using normal or gene-manipulated ES cells have helped to elucidate the process of normal embryogenesis and the genetic mechanisms of some diseases (Lensch and Daley, 2006).

Hematopoietic and endothelial development are regarded as particularly good processes for comparing the potential of ES cells cultivated in vitro with those grown in vivo (Nakano et al., 1994, 1996; Nishikawa et al., 1998). During embryogenesis, the developmental progression to a hematopoietic lineage is closely associated with progression to an endothelial lineage (Shalaby et al., 1997; Wood et al., 1997; Choi et al., 1998; Garcia-Porrero et al., 1998). Both cell lineages emerge from common mesodermal progenitors called hemangioblasts, which are positive for the vascular endothelial growth factor receptor Flk-1 (Flamme et al., 1995; Risau, 1995; Risau and Flamme, 1995; Choi et al., 1998; Huber et al., 2004). Thereafter, the site of hematopoiesis shifts from the yolk sac (primitive hematopoiesis) to the fetal liver, the spleen, and finally to the bone marrow (definitive hematopoiesis), and is accompanied by a change in the type of hemoglobin produced by erythrocytes (Moore and Metcalf, 1970; Matsuoka et al., 2001). Orderly hematopoietic development can be induced from murine and primate ES cells by various culture methods (Doetschman et al., 1985; Leder et al., 1985, 1992; Nakano et al., 1994, 1996; Xu et al., 2001; Umeda et al., 2004, 2006; Shinoda et al., 2007).

ES cells have been proposed as a potential new source of transplantable cells in regenerative medicine. It is anticipated that in the future such ES-derived cells may be used as sources of hematopoietic cells for stem cell transplants, or of mature blood cells for transfusion therapies. Recent studies have already shown that hematopoietic cells derived from murine ES cells overexpressing HoxB4 or Stat5 can replenish the bone marrow of lethally irradiated recipient mice (Kyba et al., 2002, 2003). However, there are various impediments to the clinical application of ES cells. For example, because they are established from the inner-cell masses of blastocysts, ES cells are subject to the controversy surrounding the manipulation of oocytes. Furthermore, the therapeutic use of ES cells from other individuals carries the risk of immunological complications.

Murine and human induced pluripotent stem (iPS) cells have recently been established from somatic cells by retrovirally introducing certain combinations of genes, such as octamer 3/4

The authors indicate no potential conflicts of interest.

Contract grant sponsor: Ministry of Education, Culture, Sports, Science, and Technology of Japan.

*Correspondence to: Toshio Heike, Department of Pediatrics, Graduate School of Medicine, Kyoto University, 54 Kawahara-cho, Shogoin, Sakyo-ku, Kyoto 606-8507, Japan.
E-mail: heike@kuhp.kyoto-u.ac.jp

Received 20 March 2009; Accepted 19 May 2009

Published online in Wiley InterScience (www.interscience.wiley.com.), 26 June 2009.
DOI: 10.1002/jcp.21864

(*Oct3/4*), sex-determining region Y-box 2 (*Sox2*), Krüppel-like factor 4 (*Klf4*), and the v-Myc avian myelocytomatosis viral oncogene homolog (*c-Myc*) (Takahashi and Yamanaka, 2006; Meissner et al., 2007; Okita et al., 2007; Park et al., 2007; Takahashi et al., 2007; Yu et al., 2007; Aoi et al., 2008; Hanna et al., 2008; Nakagawa et al., 2008). The cloned cells display properties of self-renewal and pluripotency similar to ES cells, and yield germ-line adult chimeras. However, because iPS cells are "unnatural" cells that are reprogrammed from once-differentiated cells, their differentiation processes must first be analyzed and compared before any true relationship between iPS and ES cells can be made.

The concept of patient-specific stem cells is of great clinical interest, and has engendered considerable research within the scientific community. The applications of these cells are expected to contribute to patient-oriented disease investigations, drug screenings, toxicology, and transplantation therapies (Jaenisch and Young, 2008). For example, a recent study demonstrated that autologous iPS cells can be used to treat mice with sickle cell anemia (Hanna et al., 2007). Despite such encouraging results, little is known about the in vitro hematopoietic differentiation of iPS cells. In particular, it is currently unclear whether iPS and undifferentiated embryonic cells follow the same process toward hematopoietic commitment.

In this study, we compared the hematopoietic differentiation of iPS and ES cells in vitro during their coculture with OP9 stromal cells (Nakano et al., 1994, 1996; Umeda et al., 2004, 2006; Vodyanik et al., 2005; Shinoda et al., 2007; Vodyanik and Slukvin, 2007). Sequential fluorescence-activated cell sorting (FACS), immunostaining, and reverse transcription (RT)-polymerase chain reaction (PCR) analyses demonstrated that iPS cell-derived hematopoietic and endothelial cells emerge from a common mesodermal progenitor that is positive for Flk-1, as is the case in ES cells and in normal embryogenesis.

Materials and Methods

Generation of iPS cells

Murine iPS cells were established from murine fibroblasts as described previously (Takahashi and Yamanaka, 2006; Okita et al., 2007; Nakagawa et al., 2008). In brief, to generate Nanog-iPS cells (clones 20D17, 38C2, and 38D2), murine embryonic fibroblasts carrying the Nanog-GFP-IRES-Puro^r reporter were incubated in retrovirus-containing supernatants for Oct3/4, Sox2, Klf4, and c-Myc for 24 h. After 2–3 weeks, clones were selected for expansion in medium containing 1.5 μg/ml of puromycin. To generate three-factor (without c-Myc) iPS cells (clone 256H18), murine tail tip fibroblasts (TTFs) were first isolated from adult *Discosoma* sp. red fluorescent protein (DsRed)-transgenic mice. Retrovirus containing supernatants for Oct3/4, Sox2, Klf4, and GFP were then added to the TTF cultures for 24 h. Four days after transduction, TTFs were replated on SIM mouse embryo-derived thioguanine and ouabain-resistant (STO)-derived feeder cells producing leukemia inhibitory factor (LIF; designated as SNL cells). Thirty days after transduction, the colonies were selected for expansion.

Maintenance of cells

The iPS cells and the murine ES cell line D3 were maintained on confluent SNL cells at a concentration of 1×10^4 cells/cm^2 in Dulbecco's modified Eagle's medium (DMEM; Sigma–Aldrich, St. Louis, MO), containing 15% fetal calf serum (FCS; Sigma–Aldrich) and 0.1 μM 2-mercaptoethanol (2ME) (Takahashi and Yamanaka, 2006; Okita et al., 2007; Nakagawa et al., 2008). OP9 stromal cells, which were a kind gift from Dr. Kodama (Osaka University, Osaka), were maintained as reported previously (Umeda et al., 2004).

Antibodies

The primary antibodies used for flow cytometric (FCM) analysis included an unconjugated anti-stage-specific mouse embryonic antigen (SSEA1) mouse monoclonal immunoglobulin M (IgM) antibody (sc-21702; Santa Cruz Biotechnology, Santa Cruz, CA), and the following anti-mouse antibodies from Becton–Dickinson (Franklin Lakes, NJ): unconjugated rat monoclonal anti-E-cadherin, rat monoclonal allophycocyanin (APC)-conjugated anti-c-kit, unconjugated rat monoclonal anti-spinocerebellar ataxia type 1 (Sca1), unconjugated rat monoclonal anti-CD31, biotin-conjugated anti-Flk-1, biotin-conjugated anti-CD34, and biotin-conjugated anti-CD45. Two secondary antibodies against the unlabeled primary antibodies were also from Becton–Dickinson: an APC-conjugated anti-mouse IgM antibody and an APC-conjugated anti-rat IgG antibody.

The primary antibodies used to immunostain the floating erythrocytes included rabbit anti-mouse embryonic hemoglobin (a gift from Dr. Atsumi, Miwa et al., 1991) and rat anti-mouse hemoglobin β (sc31116; Santa Cruz Biotechnology). Cy3-conjugated goat anti-rabbit or anti-rat antibodies (Jackson ImmunoResearch Laboratories, Inc., West Grove, PA) were used as secondary antibodies.

The primary antibodies for immunostaining endothelial cells included anti-mouse antibodies from BD (Becton–Dickinson), an unconjugated anti-VE-cadherin rat monoclonal antibody, an unconjugated anti-CD31 rat monoclonal antibody, and an anti-eNOS rat monoclonal antibody. Horseradish peroxidase (HRP)-conjugated goat anti-rat antibodies (Jackson ImmunoResearch Laboratories, Inc.) were used as secondary antibodies.

Cytostaining

Floating cells were centrifuged onto glass slides using a Shandon Cytospin® 4 Cytocentrifuge (Thermo, Pittsburgh, PA), and analyzed by microscopy after staining with May–Giemsa, myeloperoxidase (MPO), or acetylcholine esterase (Maherali et al., 2007). Staining was performed as described previously (Jackson, 1973; Yang et al., 1999; Xu et al., 2001). For immunofluorescence staining, cells fixed with 4% paraformaldehyde (PFA) were first permeabilized with phosphate-buffered saline (PBS) containing 5% skimmed milk (Becton–Dickinson) and 0.1% Triton X-100, and then incubated with primary antibodies against embryonic or β-major globins, followed by incubation with Cy3-conjugated secondary antibodies. Nuclei were counterstained with 4,6-diamidino-2-phenylindole (Sigma–Aldrich). Fluorescence was detected and images obtained with an AxioCam photomicroscope (Carl Zeiss Vision GmbH, Hallbergmoos, Germany).

FACS

The adherent cells were treated with 0.25% trypsin/ethylenediaminetetraacetic acid (EDTA) and harvested. They were incubated in a new tissue-culture dish (Becton–Dickinson) for 30 min to eliminate adherent OP9 cells (Suwabe et al., 1998). Floating cells were then collected and stained with primary antibodies, followed by incubation with APC-conjugated anti-mouse IgM or anti-rat IgG antibodies. Dead cells were excluded by propidium iodide (Kyba et al., 2002, 2003) staining. Samples were analyzed using a FACSCalibur and Cell Quest software (Becton–Dickinson). Cell sorting with the Flk-1 antibody was performed using a FACSVantage flow cytometer (Becton–Dickinson).

Differentiation of iPS and ES cells

For initial differentiation, iPS or ES cells were treated with 0.25% trypsin/EDTA (Gibco, Grand Island, NY) and transferred onto semi-confluent OP9 cell layers at a concentration of 6×10^3 cells/cm^2 in α-minimum essential medium (α-MEM;

Gibco) supplemented with 10% FCS and 5×10^{-2} μM 2ME and without LIF. After 5 days, the induced cells were treated with 0.25% trypsin/EDTA, and 1.2×10^4 total cells/cm^2 or 1.2×10^3 sorted Flk-1$^+$ cells/cm^2 were transferred onto fresh semi-confluent OP9 cell layers, and cultured thereafter for hematopoietic differentiation in α-MEM supplemented with 10% FCS, 5×10^{-2} μM 2ME, and the following four recombinant growth factors: 100 ng/ml mouse stem-cell factor (mSCF), 4 ng/ml human thrombopoietin (hTPO), 20 ng/ml mouse interleukin 3 (mIL3), and 2 U/ml human erythropoietin (hEPO). These cytokines were kindly provided by Kirin Brewery (Tokyo, Japan).

RNA extraction and RT-PCR analysis

RNA samples were prepared using silica gel membrane-based spin-columns (RNeasy Mini-Kit™; Qiagen, Valencia, CA) and subjected to RT with a Sensiscript-RT Kit™ (Qiagen). All procedures were performed following the manufacturer's instructions. For RT-PCR, yields were adjusted by dilution to produce equal amounts of the glyceraldehyde-3-phosphate dehydrogenase (GAPDH) amplicon. Complementary DNA (cDNA) templates were initially denatured at 94°C for 5 min, followed by 29–35 amplification reactions consisting of 94°C for 15 sec (denaturing), 55–64°C for 15 sec (annealing), and 72°C for 30 sec (extension), with a final extension at 94°C for 7 min. The oligonucleotide primers were as follows: *GAPDH*, 5′-TCC AGA GGG GCC ATC CAC AGT C-3′ and 5′-GTC GGT GTG AAC GGA TTT GGC C-3′ (Baba et al., 2007a); *Rex1*, 5′-AAA GTG AGA TTA GCC CCG AG-3′ and 5′-TCC CAT CCC CTT CAA TAG CA-3′ (Baba et al., 2007a); *Brachyury*, 5′-CAT GTA CTC TTT CTT GCT GG-3′ and 5′-GGT CTC GGG AAA GCA GTG GC-3′ (Ku et al., 2004); *Flk-1*, 5′-CAC CTG GCA CTC TCC ACC TTC-3′ and 5′-GAT TTC ATC CCA CTA CCG AAA G-3′ (Baba et al., 2007a); *Scl*, 5′-ATG GAG ATT TCT GAT GGT CCT CAC-3′ and 5′-AAG TGT GCT TGG GTG TTG GCT C-3′ (Baba et al., 2007a); *Myb*, 5′-CAC CAT TCT GGA CAA TGT TAA GAA C-3′ and 5′-GTA AGG TAG GTG CAT CTA AGC-3′; *Tie1*, 5′-ATA CCC TAG ACT GGC AAG AG-3′ and 5′-TTT TGA CAC TGG CAC TGG A-3′; *Gata1*, 5′-GCT GAA TCC TCT GCA TCA AC-3′ and 5′-TAG GCC TCA GCT TCT CTG TA-3′ (Shimizu et al., 2001); *Gata2*, 5′-GCA ACA CAC CAC CCG ATA CC-3′ and 5′-CAA TTT GCA CAA CAG GTG CCC-3′ (Shimizu et al., 2004); *ε-globin*, 5′-GGA GAG TCC ATT AAG AAC CTA GAC AA-3′ and 5′-CTG TGA ATT CAT TGC CGA AGT GAC-3′ (Hansen et al., 1982); *ζ-globin*, 5′-GCT CAG GCC GAG CCC ATT GG-3′ and 5′-TAG CGG TAC TTC TCA GTC AG-3′ (Leder et al., 1985); *α-globin*, 5′-CTC TCT GGG GAA GAC AAA AGC AAC-3′ and 5′-GGT GGC TAG CCA AGG TCA CCA GCA-3′ (Nishioka and Leder, 1979); *β-globin*, 5′-CTG ACA GAT GCT CTC TTG GG-3′ and 5′-CAC AAC CCC AGA AAC AGA CA-3′ (Konkel et al., 1978); *Oct3/4* (Tg), 5′-AAA AAG CAG GCT CCA CCT TCC CCA TGG CTG GAC ACC-3′ and 5′-AGA AAG CTG GGT TGA TCA ACA GCA TCA CTG AGC TTC-3′ (Takahashi and Yamanaka, 2006); *Sox2* (Tg), 5′-AAA AAG CAG GCT TGT ATA ACA TGA TGG AGA CGG-3′ and 5′-AGA AAG CTG GGT TTC ACA TGT GCG ACA GGG GCA GT-3′ (Takahashi and Yamanaka, 2006); *c-Myc* (Tg), 5′-CAC CAT GCC CCT CAA CGT GAA CTT CAC C-3′ and 5′-TTA TGC ACC AGA GTT TCG AAG CTG TTC G-3′ (Takahashi and Yamanaka, 2006); *Klf4* (Tg), 5′-CAC CAT GGC TGT CAG CGA CGC TCT GCT C-3′ and 5′-ACA TCC ACT ACG TGG GAT TTA AAA-3′ (Takahashi and Yamanaka, 2006).

Real-time quantitative RT-PCR analysis

Forward and reverse primers for *Rex1* and *Flk-1* and the fluorogenic probes were designed according to PerkinElmer guidelines (Primer Express Software; PerkinElmer Life and Analytical Sciences, Boston, MA, http://www.perkinelmer.com), and those of *Brachyury* and *Scl* were described in a previous report (Nakanishi et al., 2009; Redmond et al., 2008). The *GAPDH* primers and probes were purchased from Applied Biosystems (Foster City, CA, http://www.appliedbiosystems.com). Quantitative RT-PCR experiments were performed using the ABI-Prism 7300 system (Applied Biosystems) following the manufacturer's instructions. Quantitative assessment of mRNA expression was performed using a GAPDH internal standard. The expression of each mRNA was compared with each day 0 mRNA expression.

The oligonucleotide primers were as follows: mouse *Rex1*, 5′-AAG CAG GAT CGC CTC ACT GT-3′ and 5′-CCG CAA AAA ACT GAT TCT TGG T-3′ (Baba et al., 2007a); mouse *Brachyury*, 5′-TAC CCC AGC CCC TAT GCT CA-3′ and 5′-GGC ACT CCG AGG CTA GAC CA-3′ (Nakanishi et al., 2009); mouse *Scl*, 5′-CAC TAG GCA GTG GGT TCT TTG-3′ and 5′-GGT GTG AGG ACC ATC AGA AAT CT-3′ (Redmond et al., 2008); mouse Flk-1, 5′-AAG CAG GAT CGC CTC ACT GT-3′ and 5′-CCG CAA AAA ACT GAT TCT TGG T-3′ (Baba et al., 2007a).

Colony-forming assay

Every other day of culture, from days 5 through 15, the adherent cells were treated with 0.25% trypsin/EDTA and harvested. They were incubated in a new tissue-culture dish (Becton–Dickinson) for 30 min to eliminate adherent OP9 cells (Suwabe et al., 1998). Floating cells were then collected and cultured at a concentration of 1×10^4 cells/ml in semi-solid α-MEM supplemented with 1.3% methylcellulose, 30% FCS, 10% bovine serum albumin, 100 μM 2ME, and a mixture of the following growth factors: 10 ng/ml human granulocyte colony-stimulating factor (hG-CSF), 2 U/ml hEPO, 20 ng/ml mIL3, 100 ng/ml mSCF, 100 ng/ml hIL6, and 10 ng/ml hTPO. Colony types were determined according to the criteria described previously (Nakahata and Ogawa, 1982a,b,c) by in situ observation using an inverted microscope. The abbreviations used for the clonogenic progenitor cells were as follows: CFU-Mix, mixed colony-forming units; BFU-E, erythroid burst-forming units; CFU-GM, granulocyte–macrophage colony-forming units; and CFU-G, granulocyte colony-forming units.

Single-cell deposition assay

The single-cell deposition assay was performed as described previously (Nishikawa et al., 1998; Umeda et al., 2006; Shinoda et al., 2007). In brief, single sorted cells were deposited in individual wells of 96-well plates with confluent OP9 layers, and cultured for 5 days in the medium described in the "Differentiation of iPS and ES Cells" Section. Each well was stained with a mixture of anti-CD45, CD41, and Ter119 rat antibodies for hematopoietic lineage detection or anti-VE-cadherin rat-antibodies for endothelial lineage detection, respectively. HRP-conjugated goat anti-rat antibodies (Jackson ImmunoResearch Laboratories, Inc.) were used as secondary antibodies.

Statistics

Statistical analyses were conducted using the Student's *t*-test or the Fisher's exact test. Statistical significance was defined as $P < 0.05$.

Results

iPS cells differentiate into hematopoietic cells in coculture with OP9 stromal cells

We initially compared iPS and ES cells by microscopic examination and FACS analysis. The Nanog-iPS cell lines (Okita

et al., 2007) (20D17, 38C2, and 38D2) were positive for green fluorescent protein (GFP) expression only when Nanog was activated. 256H18, which was established by introducing only Oct3/4, Sox2, and Klf4, expressed DsRed (Nakagawa et al., 2008) constitutively. The pMx-GFP retrovirus was introduced into this clone as a silencing indicator. The control D3 ES cells were constitutively positive for GFP. All four of the iPS clones formed ES-like colonies over more than 15 passages (Fig. 1A). The FACS analysis revealed that all of the clones expressed SSEA1, E-cadherin, and CD31 (Fig. 1B), thus demonstrating the phenotypic similarity between iPS and ES cells.

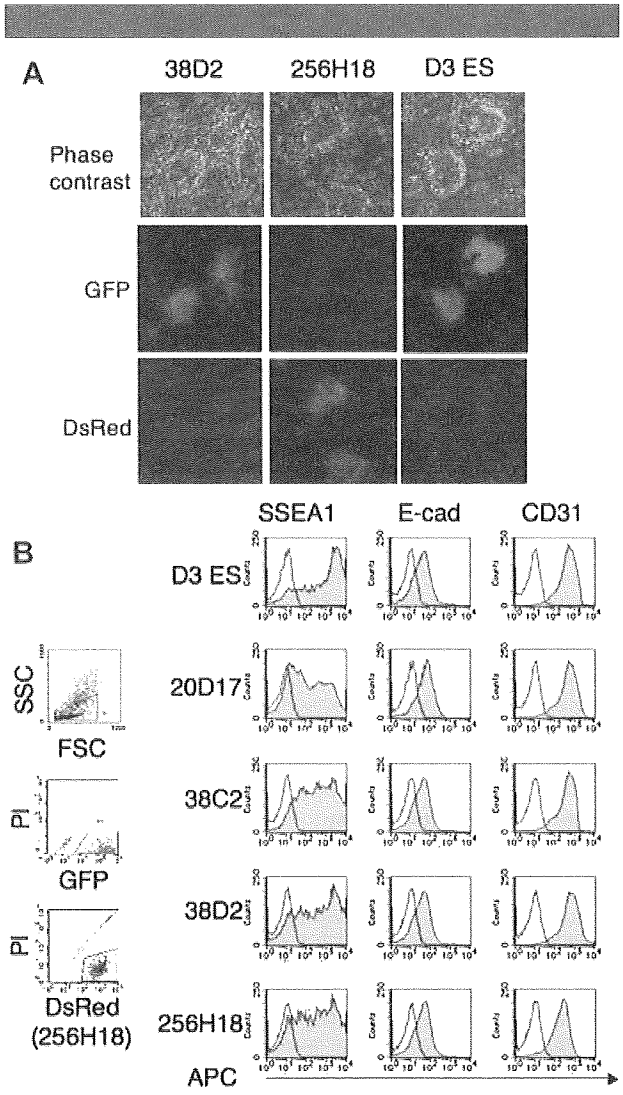

Fig. 1. Formation of ES-like colonies from iPS cells. A: Phase contrast (top row) and fluorescence (middle row: GFP, bottom row: DsRed) micrographs of Nanog-iPS cells (38D2), three-factor (without Myc) iPS (256H18) cells, and D3 ES cells maintained on SNL feeder cells. The D3 ES cells were derived from GFP$^+$ mice. Nanog-iPS cells express GFP only in the undifferentiated state. The three-factor iPS cells were derived from DsRed$^+$ mice, with additional infection by the pMx-GFP virus as a silencing marker. B: FACS analysis showing the phenotypic similarity of iPS and ES cells. The left parts show the gates for eliminating dead cells and contaminated feeders. GFP$^+$PI$^-$ cells (R2) and DSRed$^+$PI$^-$ cells (R4) were gated as ES- and iPS-derived viable cells, respectively. SSEA1, E-cadherin, and CD31 were positive in all strains (shaded bars). Open bars show staining with isotype control antibodies. Representative results from one of three independent experiments performed are presented.

To analyze the hematopoietic differentiation potential of iPS cells, we adapted the OP9 coculture system originally reported by Nakano et al. (1994, 1996). We cocultured iPS cells with OP9 stromal cells for 5 days and transferred the entire culture onto fresh OP9 layers in the presence of mSCF, mIL3, hTPO, and hEPO. Small, round cell colonies first appeared 2 days later (on day 7; Fig. 2A). These colonies gradually grew in both size and number, and a few exhibited areas with a cobblestone-like appearance. Floating cells also appeared on day 7 and thereafter. May–Giemsa staining of the floating cells on day 15 revealed enucleated red blood cells, macrophages, granulocytes, and megakaryocytes (Fig. 2B). The presence of granulocytes and megakaryocytes was confirmed by MPO and acetylcholine esterase (Maherali et al., 2007) staining, respectively. FACS analysis on day 15 confirmed the existence of various types of blood cells, including erythoid and myeloid lineage cells, but not of lymphoid lineage cells (Fig. 2C). These above results demonstrate that iPS cells, like ES cells, can produce hematopoietic cells of various lineages in vitro.

Efficient production of hematopoietic cells from sorted Flk-1$^+$ cells

To thoroughly investigate iPS cell-derived hematopoietic development, we analyzed the expression of Flk-1, a marker of hemoangiogenic progenitors. Although the proportion of Flk-1$^+$ cells in the iPS clones on day 5 varied between 20 ± 2% and 48 ± 9% (Fig. 3A), the temporal patterns of expression were similar in iPS and ES cells. No Flk-1$^+$ cells were detected at

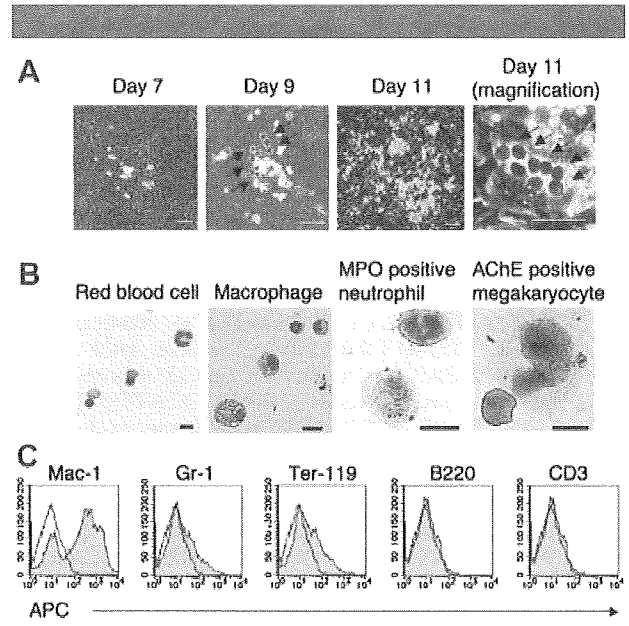

Fig. 2. Hematopoietic cells develop from iPS cells on OP9 feeders. Data from clone 38D2 are shown as representative of iPS-derived hematopoiesis. A: Small colonies first appeared on day 7 (2 days after Flk1$^+$ sorting) and then grew larger. Dark, round hematopoietic progenitors (indicated by arrows) appeared on days 9 and 11, lying beneath the OP9 layer and presenting cobblestone-like areas. Scale bars, 200 μm (left three parts) and 100 μm (rightmost part). B: Floating cells on day 15 included various lineages of hematopoietic cells; enucleated red blood cells, macrophages, MPO$^+$ neutrophils, and AChE$^+$ megakaryocytes were observed. Scale bars, 50 μm. C: Expression of lineage-specific antigens. Floating cells on day 15 were stained with antibodies against macrophages (Mac-1), granulocytes (Gr-1), erythrocytes (Ter-119), B cells (B220), and T cells (CD3). Expression of each antigen (shaded bars) was analyzed using FACS. Open bars show staining with isotype control antibodies.

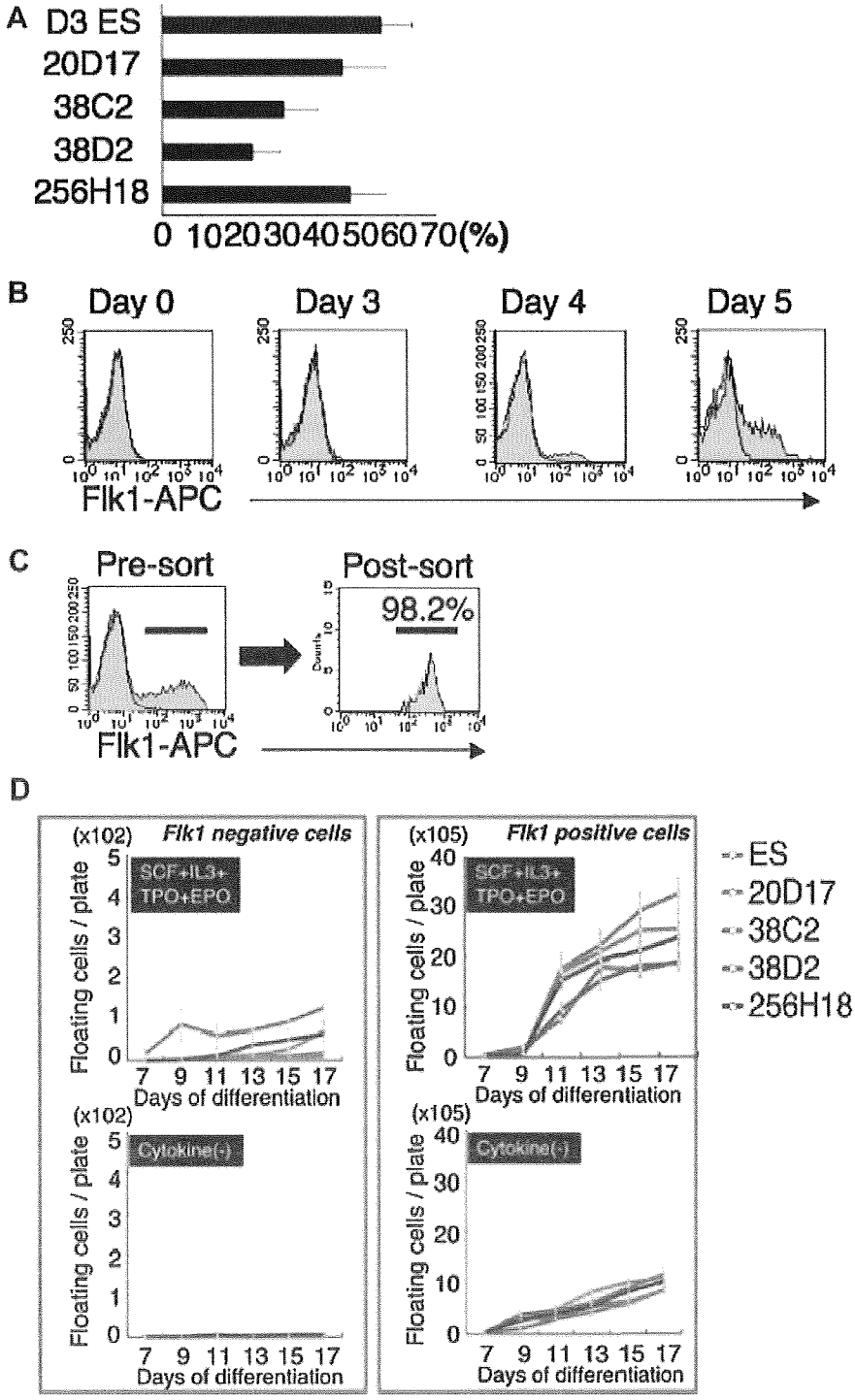

Fig. 3. Efficient production of hematopoietic cells from Flk-I$^+$ populations. A: The amounts of Flk-I$^+$ cells generated from ES and iPS cells at day 5 of differentiation were analyzed by FACS after eliminating OP9 stromal cells as described in Materials and Methods Section. Data are shown as a percentage in the total ES- and iPS-derived viable cells. B: Sequential FACS analysis reveals the emergence of Flk-I$^+$ population after day 4 of differentiation (shaded bars). Open bars show staining with isotype control antibodies. C: Purification of Flk-I$^+$ fractions by FACS on day 5. Reanalysis of the sorted cells confirmed the purity as 93.0–98.2%. D: Sequential analysis of the number of floating cells from ES and iPS cells after sorting with Flk-I antibody. Sorted Flk-I$^+$ and Flk-I$^-$ cells were cultured in the presence or absence of SCF, IL-3, TPO, and EPO. In (A) and (D), data are presented as mean ± SE of three independent duplicate experiments. In (B) and (C), representative data from clone 38D2 are shown.

the outset, but they appeared on day 4 of culture and increased in number until day 5 (Fig. 3B).

We next sorted the Flk-1$^+$ cells on day 5 and cocultured them with fresh OP9 cells. Reanalysis of the sorted Flk-1$^+$ cells by FACS showed that their purity ranged from 93.0% to 98.2% (Fig. 3C). Regardless of the percentage of Flk1$^+$ cells before sorting, all of the iPS cell lines and ES cells could produce similar yields of hematopoietic cells predominantly from Flk-1$^+$ fractions, and exogenous cytokines increased the hematopoietic efficacy fourfold (Fig. 3D).

Primitive and definitive hematopoietic development of iPS cells

In the developing mouse embryo, primitive hematopoiesis originates in the extra-embryonic yolk sac on day 7.5 of gestation (Moore and Metcalf, 1970). Thereafter, definitive hematopoiesis emerges as a second wave in the aorta-gonad-mesonephros (AGM) region and replaces primitive hematopoiesis (Muller et al., 1994; Medvinsky and Dzierzak, 1996; Matsuoka et al., 2001). Primitive and definitive erythrocytes are morphologically distinguishable, and show distinct patterns of hemoglobin gene expression: the former are larger, nucleated cells that express not only embryonic ε-globin and ζ-globin but also adult α-globin, whereas the latter are smaller, enucleated cells expressing only adult α-globin and β-globin (Doetschman et al., 1985; Leder et al., 1992; Nakano et al., 1996; Xu et al., 2001).

To investigate whether primitive and definitive erythropoiesis can occur in iPS cells, we initially examined floating hematopoietic cells (Fig. 4A). May–Giemsa staining revealed that on day 7 the cells were large and nucleated, resembling primitive erythrocytes, whereas on day 15 they were smaller, enucleating or enucleated, and similar to definitive erythrocytes. Immunostaining revealed that day 7 cells were strongly positive for embryonic hemoglobin but negative for β-major hemoglobin, while day 15 cells expressed β-major hemoglobin strongly, with little or no expression of embryonic hemoglobin.

We also examined globin gene expression in the floating cells by sequential RT-PCR (Fig. 4B). The expressions of ε-globin and ζ-globin were strongest on day 7, decreased thereafter until day 11, and were undetectable on days 13–17. In contrast, α-globin and β-major globin expression were observed from days 9 through 17. These expression patterns were similar in iPS and ES cells, suggesting that iPS cells in vitro, like ES cells, can undergo primitive followed by definitive erythropoiesis.

Hematopoietic stem/progenitor cells develop from iPS-derived Flk-1$^+$ cells

To verify the formation of hematopoietic stem/progenitor cells in our culture system, we initially examined the expressions of c-kit, Sca1, CD34, and CD45, which are expressed by early hematopoietic progenitors (van de Rijn et al., 1989; Motro et al., 1991; Ling and Neben, 1997). FACS analysis revealed that undifferentiated iPS and ES cells expressed c-kit and Sca1, but not CD34 or CD45. Subsequent examination revealed the transient downregulation of Sca1 and c-kit on day 3, with Sca1 expression increasing again on day 5. On day 13 (8 days after cell sorting), we detected a new cell population that was positive for c-kit, Sca1, CD34, and CD45 (Fig. 5A,B).

We next investigated whether clonogenic hematopoietic cells were also produced in our culture system. Methylcellulose colony-forming assays showed that CFU-Mix, BFU-E, CFU-GM, and CFU-G colonies, as described in Materials and Methods Section, developed from the iPS-derived cells (Fig. 5C), and their numbers were not much lower than those formed by ES-derived cells (Fig. 5D). CFU-Mix and BFU-E colonies predominated the Flk-1$^+$ cells on days 7 and 9, but then

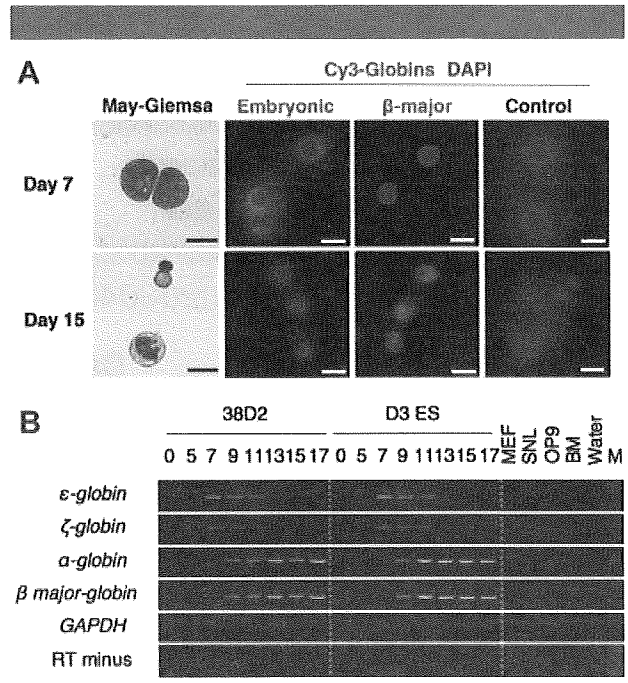

Fig. 4. Primitive and definitive erythrocytes formed from iPS cells. A: iPS-derived floating hematopoietic cells on day 7 (upper row) and day 15 (lower row) are shown. Erythrocytes on day 7 were larger and nucleated, and strongly positive for embryonic hemoglobin, but negative for β-major globin. Red blood cells on day 15 were smaller and enucleating or enucleated, and positive for β-major globin. B: Sequential RT-PCR analysis of globin gene expressions. RNA was isolated from all cells during the initiation culture (days 0 and 5), and from floating cells during the hematopoietic culture (day 7 and thereafter). GAPDH was used as a loading control. MEF, murine embryonic fibroblasts; SNL, SNL feeder cells; OP9, OP9 feeder cells; BM, adult murine bone marrow; M, 200-bp size marker. Representative results are shown from one of three independent experiments performed on clone 38D2.

decreased; the majority of cells after day 11 were from the CFU-GM and CFU-G colonies. These results suggest that iPS cells can generate multipotent hematopoietic progenitors almost as efficiently as ES cells.

Concomitant development of endothelial cells from iPS-derived Flk-1$^+$ cells

We next evaluated the development of endothelial lineages in our system. At 5 days after sorting, sheet-like colonies appeared that took up Dil-acetylated low-density lipoprotein (Dil-Ac-LDL) and were positive for anti-endothelial nitric oxide synthase (eNOS), CD31, and VE-cadherin (Fig. 6A). As shown in Figure 6B, iPS-derived Flk-1$^+$ cells produced many more VE-cadherin$^+$ colonies than Flk-1$^-$ cells ($P < 0.05$).

We also analyzed the expression of the following genes that are associated with the development of hematopoietic and endothelial lineages (Fig. 6C): required for excision 1 (*Rex1*; undifferentiated cells), *Brachyury* (primitive streak and mesoderm), *Flk-1* (mesoderm), GATA-binding protein 2 (*GATA2*; hematopoietic and endothelial), *SCL* (hematopoietic), *Myb* (hematopoietic), *GATA1* (hematopoietic), and tyrosine kinase with Ig-like and endothelial growth factor-like domains 1 (*Tie1*; endothelial). Both ES and iPS cells expressed *Rex1* strongly in the undifferentiated state. *Rex1* expression gradually decreased during differentiation, and *Brachyury*, *Flk-1*, and *SCL* expressions initially appeared on day 3. Quantitative real-time PCR analyses confirmed that *Brachyury* expression increased to

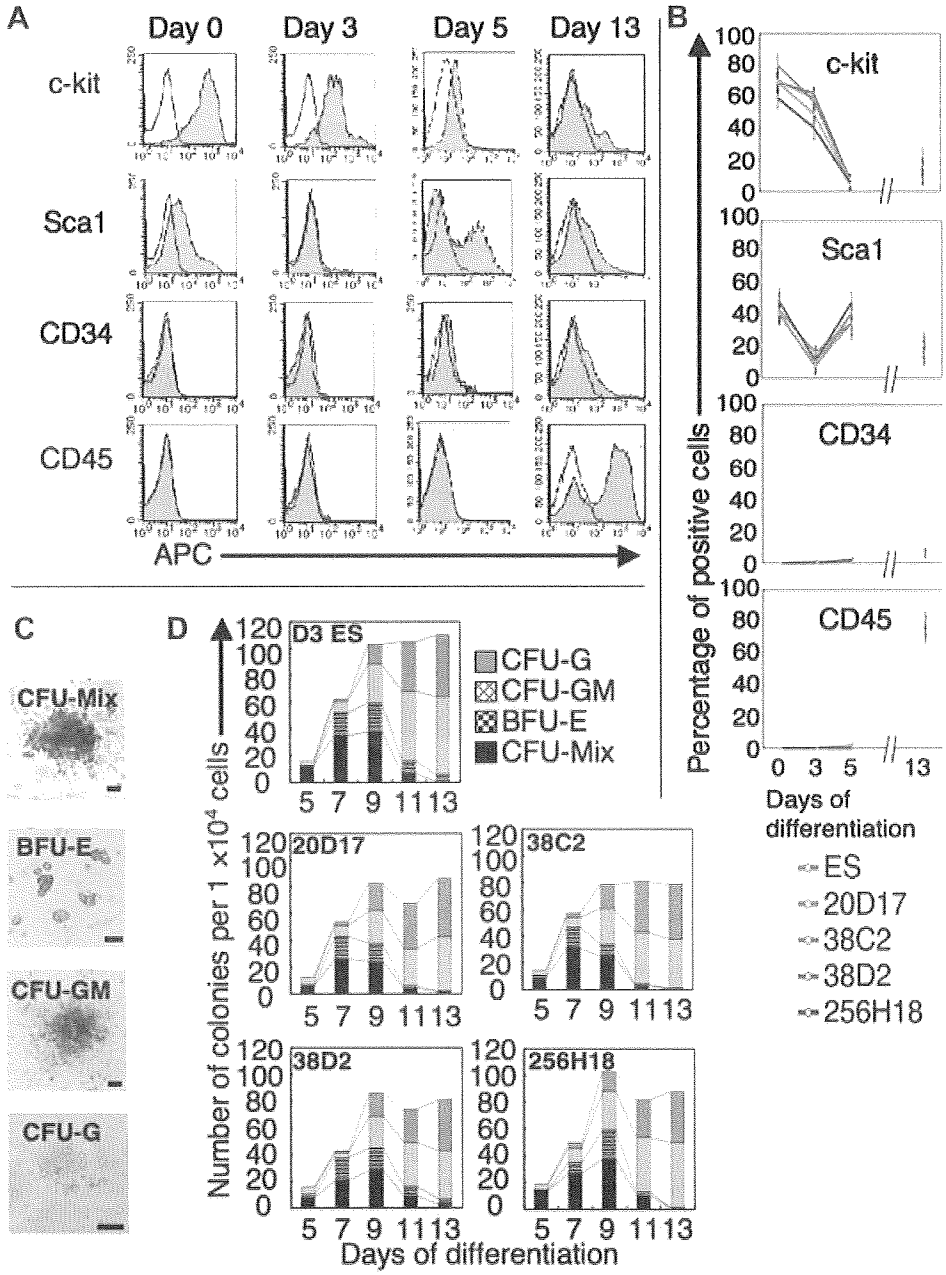

Fig. 5. Hematopoietic stem/progenitor cells emerge from Flk-1$^+$ cells. Sequential FACS analysis of c-kit, Sca1, CD34, and CD45 in ES and iPS-derived cells during differentiation. Whole culture were harvested on indicated days and analyzed by FACS as described in Materials and Methods Section. A: Representative data from clone 38D2 are shown. Histograms show the isotype control staining profile (open bars) versus the specific antibody staining profiles (shaded bars). B: Percentages of each antigen positive cells generated from ES and iPS cells are presented as mean ± SE of three independent duplicate experiments. C: The iPS cells formed various colony types on MTC-containing medium. Data from clone 38D2 are shown as representative. Scale bars, 200 μm. D: Numbers of each colony type derived from ES and iPS cells. Data represent mean of three independent triplicate experiments.

a maximum on day 3, followed by the upregulation of *Flk-1* and *SCL* (Fig. 6D). *Brachyury* expression continued until day 7, whereas that of *Flk-1* and *SCL* could be detected until day 9. *GATA2*, *Myb*, *GATA1*, and *Tie1* expressions were initially detected on day 5, and persisted thereafter. Taken together, these results demonstrate that, in our system, hematopoietic and/or endothelial differentiation of iPS cells occurs in a similar manner to that observed during embryogenesis.

Common hemoangiogenic progenitors are present in iPS-derived Flk-1$^+$ populations

Previous work has demonstrated that common hemoangiogenic progenitors are present in Flk-1$^+$ cells during ES-cell differentiation (Nishikawa et al., 1998). To investigate whether iPS-derived Flk-1$^+$ cells possess the same differentiation potential, we performed a single-cell deposition

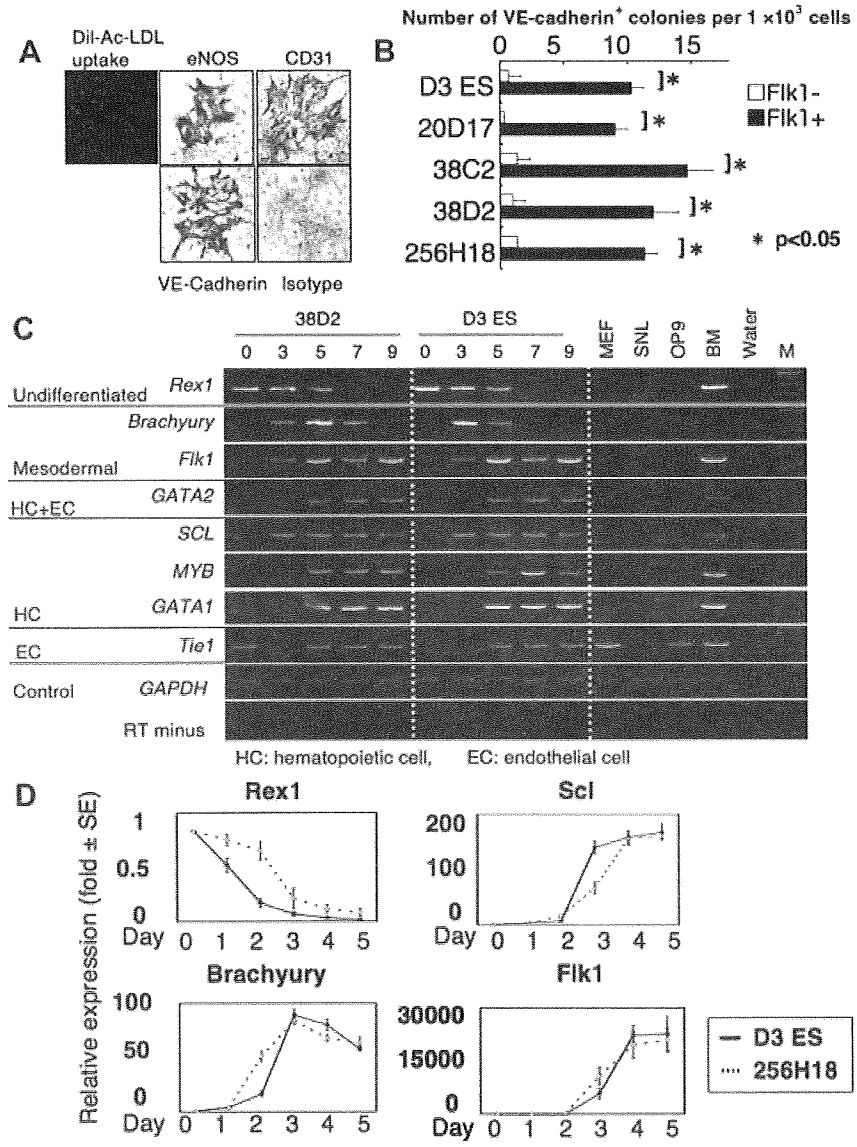

Fig. 6. Concomitant endothelial and hematopoietic development from iPS-derived Flk-1$^+$ cells. A: The sheet-like colonies took up Dil-Ac-LDL and were positive for eNOS, CD31, and VE-cadherin. Data from clone 38D2 are shown as representative. B: Number of VE-cadherin$^+$ colonies per 1×10^3 Flk1$^+$ or Flk1$^-$ cells derived from ES and iPS cells. Data are presented as mean ± SD of three independent experiments. C: RT-PCR using mRNA isolated from ES and iPS-derived cells during culture. HC and EC means hematopoietic and endothelial cells, respectively. GAPDH was used as a loading control. M: 200 bp size marker. Representative results from one of three independent experiments performed on clone 38D2 are shown. D: The expressions of *Rex1*, *Brachyury*, *Scl*, and *Flk-1* were evaluated by real-time quantitative RT-PCR. mRNA samples were harvested from D3 ES-derived GFP$^+$ cells or clone 256H18-derived DsRed$^+$ cells sorted by FACS on indicated days. Values were normalized to *gapdh* mRNA, and the control values were arbitrarily set to day 0 (undifferentiated ES cells). Data represent the mean ± SE of three independent duplicate experiments.

assay using the DsRed$^+$ clone 256H18. Single Flk-1$^+$ cells were deposited in four 96-well culture dishes (384 wells) containing OP9 feeder cells. Each well was observed by fluorescence microscopy 24 h after cell deposition, and wells that contained more than one DsRed$^+$ cell were excluded from further analysis. The presence of hematopoietic (Woodard et al., 2000) and endothelial (Maherali et al., 2007) colonies was confirmed not only morphologically, but also by immunostaining with a mixture of anti-CD41, CD45, and Ter119 antibodies, and anti-VE-cadherin antibodies, respectively, as previously reported (Fig. 7A) (Nishikawa et al., 1998). After 5 days of culture, the clonal outgrowth rates were 10.2% and 8.9% from 256H18 iPS and D3 ES cells, respectively. The frequencies of EC development alone, HC development alone, and HC plus EC development, respectively, were 2.7%, 5.2%, and 2.2%, respectively, from iPS cells and 2.4%, 3.5%, and 2.9%, respectively, from ES cells (Fig. 7B). Thus, the potential for mono- or bipotential progenitor development from iPS cells was almost equivalent to that from ES cells.

Discussion

Induced PS cells may serve as a novel cell source in both research and the clinic because, like ES cells, they have an